We are IntechOpen,
the world's leading publisher of
Open Access books
Built by scientists, for scientists

6,900
Open access books available

186,000
International authors and editors

200M
Downloads

Our authors are among the

154
Countries delivered to

TOP 1%
most cited scientists

12.2%
Contributors from top 500 universities

CLARIVATE ANALYTICS
BOOK CITATION INDEX
INDEXED

WEB OF SCIENCE™

Selection of our books indexed in the Book Citation Index
in Web of Science™ Core Collection (BKCI)

Interested in publishing with us?
Contact book.department@intechopen.com

The Structure of Supported Ionic Liquids at the Interface

Fatemeh Moosavi

Additional information is available at the end of the chapter

1. Introduction

Ionic liquids (ILs) may acceptably be defined as fluid semi-organic salts composed entirely of bulky asymmetric organic cations and organic or inorganic anions at or near room temperature. There is considerable consensus that a qualified IL must melt below 100 °C. Ionic liquids are salt, existing in the liquid phase at and around 298 K. A typical IL with a bulky organic cation (e.g., N-alkylpyridinium, N-N-dialkylimidazolium, alkylimidazolium, alkylphosphonium, and alkylammonium) is weakly coordinated to an organic or inorganic anion, such as BF_4^-, Cl^-, I^-, $AlCl_4^-$, PF_6^-, NO_3^-, CH_3COO^-, $CF_3SO_3^-$, $[(CF_3SO_2)_2N^-]$, etc. to constitute a series of low melting ILs, as shown in Figure 1.

Common Cations:

R4—N⁺—R2 (R1, R3) — Tetraalkylammonium

Di, Tri, and Tetraalkylimidazolium (R1, R2, R3, R4)

Alkylpyridinium (R1)

Dialkylpyrrolidinium (R1, R2)

Dialkylpiperidinium (R1, R2)

Tetraalkylphosphonium (R1, R2, R3, R4)

Trialkylsulfonium (R1, R2, R3)

Common Anions:

BF_4^-, $B(CN)_4^-$, $CH_3BF_3^-$, $CH_2CHBF_3^-$, $CF_3BF_3^-$, $C_2F_5BF_3^-$, $n\text{-}C_3F_7BF_3^-$, $n\text{-}C_4F_9BF_3^-$, PF_6^-, $CF_3CO_2^-$, $CF_3SO_3^-$, $N(SO_2CF_3)_2^-$, $N(COCF_3)(SO_2CF_3)^-$, $N(SO_2F)_2^-$, $N(CN)_2^-$, $C(CN)_3^-$, SCN^-, $SeCN^-$, $CuCl_2^-$, $AlCl_4^-$, $F(HF)_{2.3}^-$ etc.
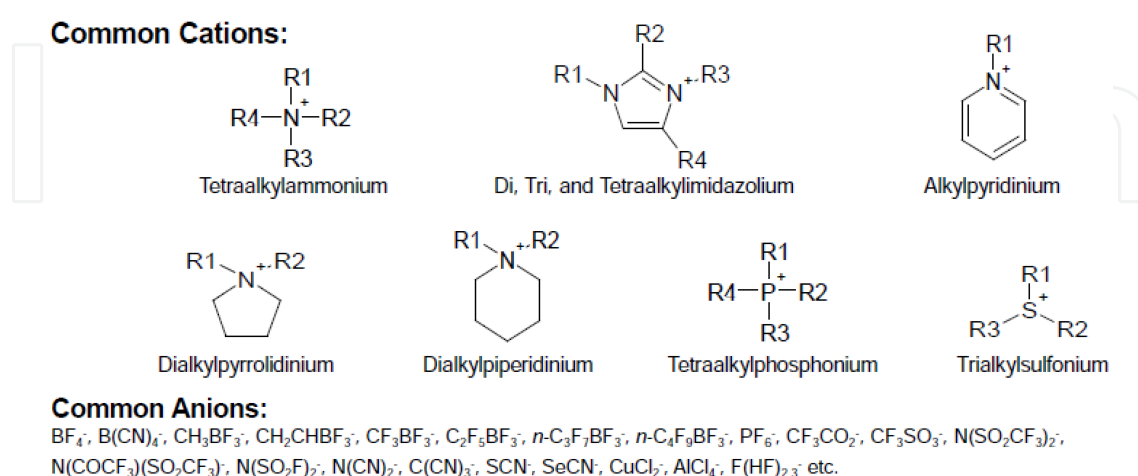
Figure 1. Common cations and anions for room temperature ionic liquids

Ionic liquids have attracted much attention as a replacement for traditional organic solvents as they possess many attractive properties. Among these properties, intrinsic ion conductivity, low volatility, high chemical and thermal stability, low vapor pressure, low combustibility, hydrophobicity, wide electrochemical windows, and high heat capacity and cohesive energy density are few. Compared with commonly used organic compounds, they have low toxicity, are non-flammable, and have negligible or nonzero volatility. Furthermore, alteration of the anions or the length of the alkyl groups allows fine-tuning of the physicochemical properties of ILs, such as viscosity, conductivity, solvation, catalytic activity, hydrophobicity, melting points, etc. Thus, ILs can be strategically designed for different applications [1,2]. The application of ILs can primarily be traced to the pioneering work in the beginning of the 1980s on pyridinium-based [3] and imidazolium-based [4] ILs for electrochemical studies. Over recent years, the concept of "green chemistry" has become well known among scientists worldwide. In particular, exploration of environmentally friendly green solvents as alternatives to volatile organic compounds in synthesis, catalysis, extraction and separation, and electrolytic processes has been persistently pursued. IL, possessing many novel properties, is the most competitive candidate that caters to all trades and professions. Properties such as nonflammability, high ionic conductivity, and electrochemical and thermal stability of ILs make them ideal electrolytes in electrochemical devices like in batteries [5-8], capacitors [9-11], fuel cells [12], photovoltaics [13-18], actuators [19], and electrochemical sensors. In addition, ILs have been widely used in electrodeposition, electrosynthesis, electrocatalysis, electrochemical capacitor, lubricants, plasticizers, solvent, lithium batteries, solvents to manufacture nanomaterials, extraction, gas absorption agents, and so forth. ILs can improve separation of complex mixtures of both polar and nonpolar compounds when used either as stationary phase or as additives in gas-liquid chromatography [20-23], liquid chromatography [22], and capillary electrophoresis [24]. They are also used in optical sensors [25,26] and also to enhance the analytical performance of the matrix-assisted laser desorption ionization mass spectrometry (MALDI-MS) [27]. The use of ILs in different applications is determined by their intrinsic properties.

To date, there have been many feature reviews dealing with different aspects of ILs, including catalysis, extraction, synthesis, nanomaterials, biosensing, energy applications, etc [28-44].

The advantages of ILs for the synthesis of conducting polymer and nanoparticle when compared to conventional media and also their electrochemical sensors and biosensors based on IL/composite modified macro-disk electrodes are the major purpose of Singh et al. in [45]. These compounds have become a novel solution to problems encountered with organic solvents and these molecules are a prospective solution to the limitations encountered in electrochemical systems [46,47]. This new chemical group can reduce the use of hazardous and polluting organic solvents due to their unique characteristics as well as taking part in various new syntheses. Due to these unique properties, ionic liquids have been widely used in different field of applications, see Figure 2.
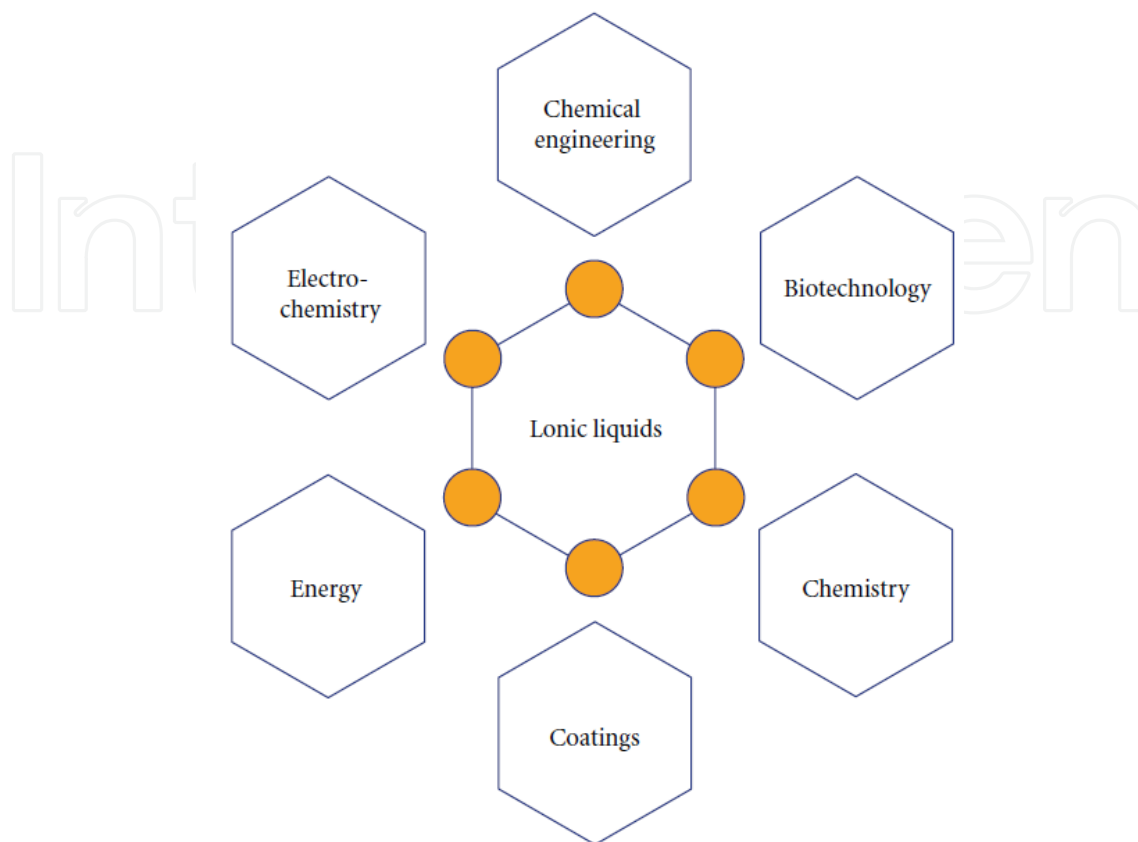
Figure 2. Applications of ILs

Considering the structural aspects of ILs, especially their surface structure on electrodes, is usually helpful for the rationalization of physical and chemical processes in ILs. The electrochemical reactions in principle are the processes at the ILs/electrode interface, including the diffusion of electroactive species, transport, capacitance at the interface, electron transfer processes etc., and which will dominate the performances in the electrochemical applications of ILs. On the other hand, the electrochemical properties in ILs are strongly dependent on the role of charge, size, polarization, and intermolecular interactions of ILs on the electrode surface. As a result, the understanding of the surface electrochemistry in ILs will benefit the performance enhancement of their application, and some novel application directions will be explored. These physical properties can be varied by selecting different combinations of ions [28,48]. Since the electrochemical window of the pure ILs depends on the electrochemical stability of the cation and/or anion, understanding the ion behavior at the electrode surface leads to improvement and implementation of the IL to the desired system [49]. The presence of an abundance of charge carriers means that when ILs are used as solvents, no supporting electrolyte is required for electrochemical experiments and this minimizes waste towards greener site [48].

2. Electrochemical supercapacitors

Supercapacitors (also called electric double-layer capacitors or ultracapacitors) are electrochemical capacitors that store energy through reversible ion adsorption onto active materials that have high specific surface area [50]. Because of their many advantageous properties, such as high power density, high capacitance, and long cycle life (>100000 cycles), these systems play an important role in electrical energy storage. To generate a high specific capacitance, the specific surface area of the electrode materials needs to be as high as possible to accommodate a large number of electrolyte ions at the electrode/electrolyte interface thereby promoting the electrical double-layer capacitance [50-52]. The latter property greatly exceeds that of conventional electrochemical energy storage devices, *e.g.*, batteries and fuel cells. Furthermore, supercapacitors can store a much greater charge per unit volume of mass than conventional dielectric-based capacitors. An electrochemical supercapacitor is based on the electrochemical double layer resulting from the electrostatic adsorption of ionic species at the electrode-solution interface, *i.e.*, no actual redox reaction is supposed to take place during the charging-discharging of these devices. To obtain the maximum possible capacitance, supercapacitor electrodes must have a high surface area; the standard material used in these devices is typically high surface area carbon. Because these devices are based on the electrosorption of ionic species, the region between the electrodes of the capacitor must contain an electrolyte with mobile ions. To obtain the maximum operating voltage without solvent decomposition, it is necessary to use aprotic solvents such as acetonitrile. Carbon-based supercapacitors based on conventional aprotic electrolytes are commercially available.

Not surprisingly, because of the numerous favorable properties described above, ionic liquids are considered promising electrolytes for electrochemical supercapacitors. $[C_2mim]BF_4$ and $[C_2mim]NTf_2$ dissolved in alkyl carbonate solvents were among the first ILs to be investigated [53]. More recently, an electrochemical supercapacitor based on *N,N*-diethyl-*N*-methyl-*N*-(2-methoxyethyl)ammonium tetrafluoroborate was shown to have superior properties compared to supercapacitors based on conventional aprotic electrolytes such as mixtures of Et_4NBF_4 in propylene carbonate [10].

An IL-based supercapacitor has even been prepared from carbon nanotubes. This device utilizes carbon gel electrodes fabricated by combining $[C_2mim]NTf_2$ with pulverized single-walled carbon nanotubes [54]. Hybrid supercapacitors obtain energy storage from the electrostatic double layer capacitance obtained at a high surface area carbon electrode and from a rapid, reversible charge-transfer process that occurs at a dopable conjugated polymer, *e.g.*, poly(3-methylthiophene) [55]. This charge-transfer process is designated as a pseudocapacitance. Not surprisingly, ionic liquids have also found their way into hybrid supercapacitors. In fact, a hybrid supercapacitor based on activated carbon, poly(3-methylthiophene), and *n*-BuMePyrNTf_2 (Pyr = pyrrolidinium) may be the first viable supercapacitor based on a IL, producing 24 Wh kg^{-1} and 14 kW kg^{-1} [56].

Graphene, a monolayer of sp^2-hybridized carbon atoms arranged in a two-dimensional lattice, has attracted tremendous attention in recent years owing to its exceptional thermal, mechanical, and electrical properties. One of the most promising applications of this material is

in polymer nano-composites, polymer matrix composites incorporating nano-scale filler materials [57]. In addition, graphene, as an atom-thick 2D nanostructure [58,59], is a promising material for supercapacitor electrodes owing to its low mass density, excellent electronic conductivity, and high surface area (~2630 m^2/g, theoretical) [60-62]. Reduced graphene oxide, RG-O, a composition closely related to graphene, is a promising material for supercapacitor applications, as specific capacitance values of 135 and 99 F/g based on RG-O-based electrodes in aqueous and organic electrolytes, respectively, have been obtained [60]. However, dispersed graphene oxide, G-O, platelets can agglomerate during reduction by, for example, hydrazine in a solvent system such as water, resulting in the possible decrease of effective surface area, resulting in a lower specific capacitance than might be expected for an ideal graphene-based supercapacitor [60]. Moreover, current supercapacitors have energy densities well below the values required to provide power assists in various applications including hybrid electric vehicles or other high energy uses [51,63]. Hence, recent efforts have been focused on the development of supercapacitors with high energy densities, which may be achieved both by enhancing the operating voltage of the devices and by improving the accessibility of the ions from the electrolyte to the active regions of electrode materials.

Toward this goal, graphene-based electrodes combined with ionic liquid electrolytes can provide an attractive alternative for supercapacitors since such combinations result in an optimal pairing of high specific surface area electrodes and wider operating potentials that may be afforded by some IL electrolytes. Generally, ILs feature moderately high ion conductivity, nonvolatility, high decomposition temperatures, and wide electrochemical stability windows, and many ILs are being considered as electrolytes to increase supercapacitor operating voltages [10,44,64,102,65]. Despite the potential of ILs as electrolytes, further work is needed to explore their potential for supercapacitors assembled with graphene-based electrodes. One of the challenges is achieving graphene-based electrode materials capable of being well wetted by the chosen ILs [51], which may be attainable by the surface modification of graphene.

Kim *et al.* have reported their progress toward high performance supercapacitors based on poly(ionic liquid)-modified RG-O electrodes and an IL electrolyte, [C$_2$mim]NTf$_2$. Poly(ionic liquid), PIL, polymers formed from IL monomers can be prepared by the polymerization of unsaturated salts. Specifically, the use of poly(1-vinyl-3-ethylimidazolium) salts bearing NTf$_2^-$ or CF$_3$SO$_2$-N-SO$_2$CF$_3$ anion has been reported to effectively stabilize hydrazine-reduced graphene oxide (RG-O) platelets *via* electrostatic and cation-π interactions, resulting in the formation of PIL-modified RG-O materials [66]. The PIL is likely physisorbed to surface of RG-O platelet and not covalently linked. These PIL-modified reduced G-O materials, PIL:RG-O, are expected to offer advantages for supercapacitor applications in that they should provide enhanced compatibility with certain IL electrolytes and improved accessibility of IL electrolyte ions into the graphene electrodes.

To investigate whether surface modification with PIL can be extended into other types of carbon electrodes, comparative experiments with the same PIL were applied to activated carbons (ACs) without RG-O platelets present. The result showed that the PIL is blocking the pores of the ACs to such an extent that the IL electrolyte cannot penetrate. For exam-

ple, the PIL-modified AC electrodes exhibited far lower specific areas as measured. Given the apparent blocking of mesopores by the PIL, it would seem that good options for electrode materials include those having relatively high aspect ratios such as conductive platelets and conductive nanorods. For example, it is reasonably likely that a good configuration for SWNTs can be found where they would be PIL-coated and combined with an appropriate IL. Other options could include 3D solids with significantly larger pore size distributions than are present in the typical activated carbon currently used in supercapacitors. The use of $[C_2mim]NTf_2$ takes advantage of its larger electrochemical stability window, allowing for operation at 3.5 V, which in turn increased both the energy density and power density of the device. To further evaluate the device performance, the frequency response of the supercapacitor incorporating the PIL: RG-O electrodes and $[C_2mim]NTf_2$ electrolyte was analyzed using electrical impedance spectroscopy (EIS). The general concept of a supercapacitor design based on PIL-modified RG-O electrodes and a compatible IL electrolyte holds potential as an electrical energy storage device indicating stable electrochemical performance and a specific capacitance as high as 187 F/g. This relatively high capacitance is presumably due to improved wettability of the chosen IL electrolyte on the PIL-modified RG-O materials which, synergistically, enhanced the effective surface area of the electrode/electrolyte interfaces.

3. Lithium-ion batteries

Lithium-ion batteries are now ubiquitous in society and serve as the power sources in almost all portable electronic devices that are marketed to today's consumer. With such widespread use and in view of the safety issue of lithium-ion batteries, there are considerable ongoing efforts by battery manufacturers to improve the performance of these devices. As a result of the many attractive aspects of ILs, there is a modest but continuing interest in using them as electrolytes for these cells. Until several years ago, the IL electrolyte of choice was some variety of chloroaluminate [67], but interest in the use of nonchloroaluminate ILs has gradually increased. It is difficult to pinpoint the first instance where nonchloroaluminate ILs were used in lithium-ion batteries. An early report describes a successful $Li/LiMn_2O_4$ cell prepared with 1,2-dimethyl-4-fluoropyrazolium tetrafluoroborate + $LiBF_4$ or $LiAsF_6$ [68]. Li/$LiCoO_2$ cells utilizing n-PrMePipNTf$_2$ (Pip = piperidinium) show good cyclic efficiency [69,70], and it is clear that ILs based on those anions that offer good anodic stability, $e.g.$, NTf$_2$- or N(SO$_2$F)$_2$-, give the best performance [70,71]. At the present time, the main problem is the incompatibility of the anode, $e.g.$, Li metal, and the ILs. That is, the solid electrolyte interphase film that is produced on the anode during the charge/discharge process is less stable than that obtained in conventional organic solvents. This incompatibility problem limits the cycling efficiency of the cell. MacFarlane $et al$. [72] have succeeded in elucidating the mechanism of film formation on Li in ILs based on N-alkyl-N-methylpyrrolidinium ions and NTf$_2^-$. Perhaps, future research of this nature will lead to resolution of this problem, enabling the practical use of ILs as electrolytes in Li batteries.

4. IL/electrode interface

By comparison of the background electrochemical behavior of an IL at both GC and platinum electrodes, one can approximately determine the amounts of protonic impurities present. The microstructure and capacitance of the electrical double layers (EDLs) at the interface of ILs and electrodes play an essential role in determining the system performance. Compared with simpler electrolytes, such as aqueous electrolytes and high-temperature molten salts, the ions in ILs are larger and often feature a complex shape. In addition, their charges are typically delocalized among many atoms [73]. Considering the solvent-free nature and the complex shape of ILs, it is expected that the classical theories for the EDLs in dilute aqueous electrolytes and high-temperature molten salts cannot accurately describe the structure and properties of the EDLs at the interface of ILs and electrified surfaces. Therefore, it is necessary to rediscover the IL/electrode interface and renew the model of IL/electrode EDLs.

Although ILs have always being investigated from the first finding in 1941 for a long period time, only a few works [74,75] concentrated on their intrinsic capacitive behaviors. A small capacitance (compared to smooth electrodes) was achieved in a practical capacitor comprising high-surface-area carbon cloth electrodes. To understand whether the observed capacitance might be due to the microporosity of the carbon cloth electrode or to the practical limitation of the device itself, the differential capacitance of 1-ethyl-3-methyl imidazolium imide IL was determined by measuring the potential of electrocapillary maximum or the point of zero charge (PZC) at an Hg electrode. The obtained capacitance at the cathodic potential is mainly determined by the cation, rather than the anion, as expected. The rate of charge, discharge, and the accessibility of electrolyte to the electrode surface ultimately determine the realizable capacitance in a practical device employing high-surface-area carbon electrodes.

The intrinsic capacitance of imidazolium-based ILs at carbon paste electrodes was investigated by using an electrochemical impedance technique [76]. The large capacitance was accounted for by intramolecular hydrogen bonding interactions that created a third charge layer between the IL and electrode EDL, which might make the interface rougher and hold more charge. The importance of ion chemistry and structure for the capacitive response of carbonaceous electrodes in ILs was stressed [77]. The double-layer capacitance of negatively charged carbon electrodes was strongly determined by the cation polarizability, which affected the dielectric constant in the double-layer, as well as double-layer thickness, which in turn also depended on the preferred orientation of the cations under the applied electric field. This suggests that the EDL constitutes a monolayer of cations up against the negatively charged carbon surface. Differential capacitance–potential curves were measured at IL/Hg, GC and Au electrode interfaces [78]. Unlike in aqueous or conventional organic solvents, capacitance–potential curves were found to vary significantly with the electrode substrates in ILs. It could be due to the absence of the inner Helmholtz layer of the molecular solvent between the electrode and ionic species, which usually works as a dominant factor in shaping the capacitance curves. The use of an electrochemical gate and ILs can reduce the

Debye ionic screen length to a few angstroms, which makes the measured capacitance nearly equal to the real quantum capacitance. The unique properties allow the direct measurement of the quantum capacitance of graphene as a function of gate potentials using a three-electrode electrochemical configuration in ILs electrolytes [79].

However, different types of ILs consist of various ions and ionic pairs structured in the bulk or IL/electrode interfaces. The bulk and interfacial behavior is governed by Columbic, van der Waals, dipole-dipole, hydrogen-bonding, and solvophobic forces [80]. The molecular organization of ILs is more complex than traditional solvents, and ILs cannot be considered as unstructured molten salts [81]. Many investigations have shown ionic liquids are nanostructured, which helps to explain their solvating power and some other unusual physical properties [82]. Spectroscopy and molecular dynamics simulation studies revealed distinct alkyl and ionic clusters in alkylimidazolium ILs [83-86]. Self-assembled IL nanostructures have also been elucidated using small-angle neutron scattering (SANS) for ILs [87], in which electrostatic contributions to solvophobicity are enhanced by the extensive hydrogen-bond network of the liquids. IL solvation layers were first detected for the ethylammonium nitrate/mica interface using surface force apparatus (SFA) [88], and subsequently detected for both protic and aprotic ILs confined between atomic force microscope (AFM) tips and mica, silica, graphite, and Au(111) [89-91]. It was found that IL nanostructures are the consequence of alkyl tail aggregation, driven by solvophobic forces inducing alkyl chains to segregate from the charged cation group and the anion, forming ionic domains. The increasing alkyl chain length leads to larger, more regular domains. The self-organized IL/substrate interfaces were observed to compose of three to seven solvation layers depending on the IL species [92]. Surface frequency generation data indicated that the interfacial cations exhibited orientational ordering and their orientation depended not only on the electrical potential of the electrode but also on the type of anions in the ILs [93]. Some experimental data suggest that the IL/electrode interface is one ion layer thick (typically 3-5 Å), which supports the idea that the EDLs in ILs are essentially Helmholtz layers [94]. Despite the lack of sufficient experimental data, two major approaches have been proposed to model the IL/electrode interface.

A molecular dynamics (MD) simulation model for an IL/metallic electrode in which the metallic electrode is maintained at a preset electrical potential is described in [95]. The model uses variable charges whose magnitudes are adjusted on the fly according to a variational procedure to maintain the constant potential condition. As such, the model also allows for the polarization of the electrode by the electrolyte, sometimes described by the introduction of image charges. The model has been implemented in a description of an electrochemical cell as a pair of parallel planar electrodes separated by the electrolyte using a two-dimensional Ewald summation method. The method has been applied to examine the interfacial structure in two ILs, consisting of binary mixtures of molten salts, chosen to exemplify the influences of dissimilar cation size and charge. The stronger coordination of the smaller and more highly charged cations by the anions prevents them from closely approaching even the negatively charged electrode. This has consequences for the capacitance of the electrode and will also have an impact on the rates of electron transfer processes. The calculated capacitan-

ces qualitatively exhibit the same dependence on the applied potential as have been observed in experimental studies.

The MD simulation study of the EDL structure near electrodes with different surface charge densities indicates that a Helmholtz-like interfacial counterion layer exists when the electrode charge density is negative or strongly positive but becomes poorly defined when the electrode charge density is weakly positive [96]. However, regardless of the presence of a distinct Helmholtz layer, the charge separation and orientational ordering of the ions persist up to a depth of 1.1 nm into the bulk ILs. The structure of the EDL is affected strongly by the liquid nature of the IL and the short-range ion-electrode and ion-ion interactions, especially at low electrode charge densities. In addition, the charge delocalization is found to affect the mean force experienced by the bulky ions near the electrode and, thus, can play an important role in shaping the EDL structure. An investigation of the electrified Au(100) surfaces in ILs by combined in situ scanning tunneling microscopy (STM) and differential capacitance measurements has revealed that the differential capacitance curves of the IL/Au interfaces have a bell-shaped feature, and ion adsorption at Au single-crystal electrodes depends critically on the structure of the surfaces [97].

The capacitance-potential (C-V) curve is virtually bell-shaped with metal electrodes in ILs composed of cations and anions of comparable size [98-101]. However, U-like C-V curves are observed at IL/nonmetallic electrode interfaces in contrast to those observed at IL/metallic electrodes [64]. The degree of curvature of the ''U-like'' curve measured at the GC electrode decreases in the ILs with low inherent ionic concentrations. The capacitance at the GC electrode exhibits a complex potential dependence, being different from those at highly oriented pyrolytic graphite (HOPG) and metal electrodes. However, in most real IL systems they are not hard and are not spheres. Therefore, long and challenging investigations to better understand IL/electrode interfaces are still ahead.

5. Other electrochemical applications

Besides the above application, ionic liquids are also used in some other electrochemical applications, such as electrochemical biosensing, electrochemical capacitors, lithium batteries, etc. Precisely, controlling the interface between the electrode and IL solvents allows scientists to alter the electron transfer and storage ability in the devices, and thus improve their performances. The details in this field have been well reviewed by other authors in references [102-104] and here is just glance at the use of ILs in these fields.

Enzyme electrodes are one of the most intensively researched biosensors because enzymes are highly selective and respond quickly to a specific substrate [105]. A new type of amperometric biosensor based on IL sol-gel material using the hydrolysis of tetraethyl orthosilicate in $[C_4mim]BF_4$ solution was reported [106]. The IL sol-gel enzyme electrodes retained the high activity of horseradish peroxidase (HRP) and provided long-term stability of HRP in storage. The uniform porous structure of the IL sol-gel matrix resulted in a fast mass transport, which provided a unique microenvironment around the enzyme, resulting in high sen-

sitivity and excellent stability of the enzyme. An interesting electrochemical biosensor towards electrocatalysis of H_2O_2 was designed by entrapping HRP in IL doped DNA network [107], in which DNA with a specific double-helix structure and stacked base pairs may afford both biocompatible microenvironments around enzymes entrapped in the membranes and an effective pathway for electron transfer. Recently, IL-based sensors have been used for trace explosive detection by integrated electrochemical and colorimetric methods [108]. The explosives are pre-concentrated in ILs first.

A recent report showed that the use of [C_4mPy]TFSI in combination with a graphite and silicon electrode could maintain good lithium cycle performance in the presence of film-forming additives, such as vinylene carbonate (VC), that served as the only source of reactive chemical for an effective SEI formation at the electrolyte/electrode interface [109]. Silicon electrodes displayed higher compatibility with [C_4mPy]TFSI compared with graphite.

The latest researches of ILs in surface electrochemistry, including the IL/electrode interface and electron transfer in ILs has been highlighted in a review by Liu *et al.* [110]. As a result, the absorption, mass transport, and electron transfer at the interfaces of ILs/electrodes are complicated and quite different to that in traditional solvents. Some experimental data suggest that the IL/electrode interface is one ion layer thick (typically 3-5 Å) showing that they are essentially Helmholtz layers. Through spectroscopic techniques, *e.g.* SFA, AFM, SFG, and SANS, ILs are recently illustrated to be nanostructured as a consequence of alkyl tail aggregation driven by solvophobic forces. In the IL medium, the mobile carrier densities are shown to be able to be determined using a simplified capacitor model in a three-electrode electrochemical system, in which the electron transport characteristics are interpreted in terms of charged impurity induced scattering [79].

These strategies give ILs great promise for applications of ultrahigh frequency electronics and for studying the intrinsic transport properties of the Dirac fermions in graphene devices. It is believed that some new application directions beyond those mentioned above will be explored with the deep understanding of the structure and composition information at the ILs/electrode interface in the near future. There is no doubt that ILs will play more important roles in the electrochemical applications in both science and technology because of their unique properties.

Ionic liquids are a good choice as binder in carbon paste electrodes due to their interesting properties, mentioned previously. Recently, ionic liquids have been widely used as efficient pasting binders instead of non-conductive organic binders in preparation of carbon composite electrodes [111].

Carbon paste electrode based on MWCNTs and ILs types of electrodes show superior performance over traditional carbon paste electrodes. Solution studies shows a selective interaction between cerium acetylacetonate complex (CAA) and monohydrogen phosphate respect to a number of anions tested, therefore, the complex was used as sensing material in construction of a HPO_4^{2-} nano-composite carbon paste sensor based on MWCNTs and ILs. A new HPO_4^{2-} nano-composite carbon paste electrode was introduced [111]. From the other side of view, the purity of the nanotubes affects the gelation.

6. Molecular-scale insights into the mechanisms of ionic liquids interactions with carbon nanotubes and graphite surfaces

Ionic liquids have shown great promise for application in heterogeneous systems, such as lubricants, heterogeneous reactions, heterogeneous catalysis, electrochemistry, and fuel cells [15,29,31,112-116]. However, for these particular applications, a more detailed understanding of the molecular structure of the interface between IL and solid is essential.

Recently, the structures of the gas-liquid and liquid/liquid interfaces of ILs have been investigated computationally [117-121] and experimentally [122-137]. Some groups have studied the structure and dynamics of ILs by analytical techniques, such as X-ray diffraction [136-137], sum-frequency generation technique, SFG, [126,127] IR and Raman spectroscopies [134,135], direct recoil spectroscopy [122], neutron reflectometry [129], etc. They have suggested that the cations lie normal to the liquid surface and a density oscillation near the surface is also evident at the vapor-liquid interface. These studies, as well as several molecular dynamics simulations [117-121], have indicated that both cations and anions are populated at the liquid surface via a specific orientation.

Compared to gas-liquid and liquid-liquid properties of ILs, efforts to investigate solid-liquid surfaces or interface structures of ILs have so far been limited [93,132,138]. Owing to possible strong interactions between ILs and solid surfaces, a transition of IL from liquid to solid may take place. Evidence [116,139,140], has already demonstrated the coexistence of liquid and solid phases of IL [C_4mim]PF_6 on mica surfaces at room temperature by using atomic force microscopy, AFM. Although it has previously been found that some liquids, e.g., water become ordered or solid-like in the layers adjacent to the surface of crystallized solid substrates [141], a solid layer of [C_4mim]PF_6 formed on mica surfaces is much more stable. Since the melting point of [C_4mim]PF_6 is ~7 °C, it is a good model for the study of liquid/solid interactions and the possible phase transformation. Moreover, it has also been observed that, when confined to multiwalled carbon nanotubes, [C_4mim]PF_6 can be transformed into a crystal with a high melting point [142]. Some other groups have also studied the interactions between solid surface and IL. For example, by using sum-frequency vibrational spectroscopy, Fitchett and Conboy [143] have reported that the alkyl chains of the imidazolium cations are nearly normal to SiO_2 surfaces for a series of hydrophobic ILs. Romero and Baldelli [144] have studied [C_4mim]PF_6 and [C_4mim]BF_4 with hydrophobic and hydrophilic properties, respectively, and shown that the imidazolium ring lies on the plane of the quartz surface with the methyl group pointing 43 °C-47 °C from normal, displaying resonances from the alkyl chain as well as the aromatic ring by using SFG. Atkin and Warr *et al.* [89] have measured the solvation force profiles for several ILs on different solid surfaces by AFM. However, there is still a lack of detailed understanding of the ordered or solid-like molecular structures of ILs at solid/liquid interfaces.

ILs have been demonstrated to be interactive toward a number of solid materials, such as single-walled carbon nanotubes (SWNTs), graphite, silica, mica, and kaolinite, through interaction mechanisms such as H-bonding, π–π stacking, Van der waals forces, electrostatic forces, and so on [145-147]. For instance, Fukushima *et al.* [146] discovered uniform SWNTs

bucky gels by grinding SWNTs in ILs, since the cation–π interaction exists between the imidazolium ion of IL and the π-electrons of the fullerene of SWNTs. In contrast, common organic solvents such as dichlorobenzene, ethanol, N, N-dimethylformamide, and 1-methylimidazole (a precursor for ionic liquids) did not form gels, even upon prolonged grinding with SWNTs. Likewise, no gelation of ionic liquids took place with other carbon allotropes such as graphite (1 to 2 μm) and C60 [148]. With all the above features in mind, rheological properties of the bucky gels of ionic liquids have been investigated in reference. SWNTs can orient imidazolium ions on their π-electronic surfaces by way of a possible "cation-π" interaction. Such a molecular ordering may trigger clustering of the surrounding imidazolium ions columbically and consequently interconnect neighboring SWNT bundles.

Lungwitz *et al.* [147] suggested that, due to the anion-silica interactions, both physisorption and chemisorptions occurred in the phase boundary of N-methylimidazolium chloride/silica. In addition, the adsorption of IL on other silicates or soils surfaces are mostly spontaneous; many adsorption mechanisms have been proposed, such as ion exchange, ion pairing, dispersive force, and so on [149]. Adsorption of IL on these solid materials indicates that these ILs could modify the surface of clay and eventually leads to significantly changed properties of both the clay and IL, such as the thermal stability, supermolecular structures [140], and crystallization behavior [142]. Halloysite nanotubes (HNTs), mined from natural deposits, are a kind of clay aluminosilicate mineral with hollow nanotubular structure and a high aspect ratio. The length of HNTs is usually in the range of 1-15 μm and the inner diameter and outer diameter of HNTs are 10-30 and 50-70 nm, respectively [150]. Halloysite, also named metahalloysite and chemically similar to kaolin, has the molecular formula $Al_2Si_2O_5(OH)_4.nH_2O$. In the pH range of 2-12, the inner and outer surfaces of HNTs are negatively charged [151] so it may absorb imidazolium cations of IL via an electrostatic effect. In addition, it was found that the outer surfaces of HNTs are mainly composed of siloxane and have only a few silanols and aluminols, which indicates that HNTs possess potential ability for the formation of hydrogen bonding with imidazolium-based ILs.

Guo and his coworkers confirmed [107], by thermogravimetric analysis, the retention of $[C_4mim]PF_6$ IL on HNTs in a tetrahydrofuran-water mixture and the formation of IL-coated HNTs (m-HNTs). In addition, the interaction was confirmed and the hydrogen bonding was proposed to as a possible mechanism. HNTs have been utilized as effective reinforcements for various polymers [152], therefore, the curing and performance of rubber compounds with m-HNTs were examined. The unique changes in the rubber compounds were correlated to the changes in filler dispersion and interaction between IL and HNTs. The IL absorbed on HNTs surface to form a mesostructure, which is different from that of the neat crystallized IL. The interaction between IL and HNTs was proposed to be hydrogen bonding and verified by the spectral results. Because of the interaction, the crystallization behavior of IL in the presence of HNTs was found to be changed. Compared with the compounds with HNTs, the uncured compounds with HNTs coated with IL showed significantly faster curing and the resulting vulcanizates showed substantially higher tensile strength and much lower hardness.

Interest in carbon nanotubes (CNTs) dispersed in ILs is rapidly growing [44,51]. One of the main reasons is the extraordinary electrochemical and bioelectrochemical properties of ILs [153] as well as of carbon nanotube composite materials. Such, CNTs/ILs have promising supercapacitor applications.

It has been shown in several experimental [89,91,92,117,154] and theoretical [98,155] studies that the molecular structure of IL ions strongly influences the IL interface properties at different charged and uncharged interfaces. For instance, Lockett *et al.* [154] showed that asymmetry in the size and shape of molecular ions results in unequal distribution of molecular cations and anions in direction normal to the IL-vacuum interface. These results suggest that the molecular structure of IL ions should make significant effects at the CNT/IL interface. However, still, there is a lack of molecular level information on the mechanisms of the IL interactions with nanocarbon electrodes.

Endres *et al.* [156] quoted an ''undoubted'' formation of at least three solvation layers of [C_2mim]TFSI on metal electrodes detected by atomic force microscopy (AFM). Recently, Hayes *et al.* [157] investigated the influence of the electric potential on the interface solvation layers in [C_2mim]FAP and [C_4mPyrr]FAP, by AFM, at the charged Au(111) electrode the support the experimental observations. They showed that IL layering is more pronounced at charged Au(111) surface compared to the neutral surface and increase of the potential leads to flattening of the tightly bound cation layer, indicating possible reorientation of cations ([C_2mim] and [Py]) to lay flat on the surface. The similar effects can be observed: increase of the potential at the CNT cathode significantly increases the tendency of [C_2mim] cation to lay flat on the surface. Applying an electric potential on the CNT electrode and/or varying the chemical structure of IL molecular ions, it is possible to change ion orientations and thus the structure of the CNT-IL interface shell.

Applying an electric potential, they found that the innermost layer changes its structure and becomes more strongly bound to the surface. At the cathode, for "the first time an interfacial (innermost) anionic layer at a solid interface has been detected by AFM". Atkin *et al.* [91] published an AFM study of the gold interface solvated in [C_2mim]TFSI and reported results which coincide well with the observed layered structure in MD simulations of neat [C_2mim]TFSI at the CNT surface performed by Frolov *et al.* [158]. They attributed the ''weaker'' layering pattern in simulations to the differences in temperatures: temperature in the simulations was about 70 °C, while "all force curves were acquired continuously at room temperature (22 °C)" for the AFM measurements.

There are some experimental studies on the orientation of IL molecules on the liquid-vacuum interface, see for example references [154,159,160]. Nakajima *et al.* [159] investigated the liquid-vacuum interface of different 1-alkyl-3-methylimidazolium-TFSI ionic liquids using high-resolution Rutherford backscattering spectroscopy. They showed that, due to their solvophobic nature, long alkyl chains of cations point away from the bulk liquid to vacuum and therefore stimulate the imidazolium ring to stay perpendicular to the surface. Simulations on the IL-carbon interface were observed an opposite effect: increase of alkyl chains increases the tendency for the imidazolium ring to lay parallel on the surface. The differences between IL-vacuum and IL-carbon nanotube interfaces to the strong Van der Waals at-

traction between the non-polar alkyl chains and carbon nanotube surface can be attributed. Contrary to the IL-vacuum interface, at the IL-CNT interface the alkyl chains of imidazolium-based cations tend to lay parallel on the CNT surface and force the imidazolium rings also to lay flat on the carbon nanotube surface.

One of the main reasons on rapidly growing interest in carbon nanotubes, CNTs, dispersed in ILs is the extraordinary electrochemical and bioelectrochemical properties of ILs as well as of carbon nanotube composite materials. Such, carbon nanotubes (nanotube forests) with ILs have promising supercapacitor applications. It has been shown in several experimental and theoretical studies that the molecular structure of IL ions strongly influences the IL interface properties at different charged and uncharged interfaces. For instance, Lockett *et al.* [161] showed that asymmetry in the size and shape of molecular ions results in unequal distribution of molecular cations and anions in a direction normal to the IL-vacuum interface. These results suggest that the molecular structure of IL ions should make significant effects at the CNT-IL interface.

Molecular simulations can provide complimentary information to the experimental data that should help to obtain a detailed picture of the interface phenomena in IL systems. Therefore, fully atomistic simulation for studying basic mechanisms of the IL interactions with the CNT surface has been applied [158]. The results have shown that ILs based on combination of imidazolium-based cations with hydrophobic anions (e.g. BF_4^- or TFSI) are moisture stable and have very promising electrochemical applications. Ion conductivity of [C_2mim]TFSI is comparable to the best of organic electrolyte solutions, and this liquid is stable up to 300-400 °C. The TFSI-based ionic liquids are practically not miscible with water but they are well miscible with several organic solvents, e.g., acetonitrile, AN [162]. The effects of the cation molecular geometry on the properties of the interface structure in the IL systems was investigated by a set of three ILs with the same anion (TFSI) but with different cations, namely, [C_2mim], [C_4mim], and [C_8mim] [158]. The cations had identical charged methylimidazolium 'heads' but different nonpolar alkyl 'tails' where the length of the tail increases from ethyl to octyl and the focus was concentrated on a set of the following questions:

- What is the interfacial structure of IL-AN mixture at the neutral CNT surface?

- How does the interfacial structure change at the positively charged CNT surface?

- How does the interfacial structure change at the negatively charged CNT surface?

- Does the length of the cation alkyl tail affect the interfacial IL-AN structure and preferred orientation of the IL ions at the CNT surface?

- What is the role of acetonitrile solvent in these interfacial effects?

Taking into account the molecular volume of the investigated ions, the probability of finding an ion inside the CNT pore was assumed to be low.

The analysis of the simulation data results in the following conclusions:

1. There is an enrichment of all molecular components of ILs under study at the CNT surface with formation of several distinct layers even at the non-charged CNT surface.

2. Mixing IL with acetonitrile decreases ion-counterion correlations in the electric double layer.

3. Increase of the length of the non-polar cation 'tail' increases propensity of imidazolium-based cations to lay parallel to the CNT surface.

4. At the CNT cathode TFSI anions and molecular cations are preferentially oriented parallel to the surface.

5. At the CNT anode the TFSI anions are oriented parallel to the surface, however the preferred orientations of cations depend on the length of non-polar tail: $[C_2mim]^+$ cations are oriented perpendicular to the surface, $[C_4mim]^+$ are in both parallel and perpendicular orientations, $[C_8mim]^+$ are oriented parallel to the surface.

6. By applying electric potential on the CNT electrode or/and varying the chemical structure of IL molecular ions it is possible to change the interfacial orientation of IL ions and, consequently, the structure of the CNT-IL interface shell.

As an effective computation technique, molecular dynamics program has been widely used for simulating interfacial phenomena. The interfacial molecular structure of $[C_4mim]PF_6$ in contact with the graphite surface has been studied for the first time at 2008 [163]. Maolin and his worker used $[C_4mim]PF_6$ as the model because it is hydrophobic and widely investigated. They investigated how the hydrophobic graphite surface affects the structure and orientation of hydrophobic $[C_4mim]PF_6$ at the interface. The MD calculation indicated the formation of a stable bottom layer, as well as possible single, double, or triple layer of $[C_4mim]PF_6$ on the graphite surface. The orientation calculations showed that the alkyl chains and imidazolium ring of cations both lie in the plane of the hydrophobic graphite surface.

Molecular dynamics simulations were performed to understand the microscopic structure of the IL $[C_4mim]PF_6$ on a graphite interface. In addition, MD simulations showed the existence of a solid-like IL bottom layer of about 6 Å thickness on the graphite surface. Compared to the bulk IL, the mass density peak of the bottom layer is 90% higher and its electron density peak is 80% higher. The butyl group and imidazolium ring of the cation of the IL bottom layer are parallel to the graphite surface. Due to the strong interactions between the cations and the graphite surface, ILs possessing longer alkyl tails and more imidazolium ring or aromatic ring may be applied to form more stable and well-regulated layers at graphite surfaces. This finding is important for the understanding of modification or lubrication mechanisms of ILs on solid surfaces, especially on the surfaces of carbon nanotubes and carbon black.

Several experimental and computational articles suggest that a possible layering of molecules in IL occur at the vapor-IL interfaces [119-121]. The influence of the vapor-IL interface on single, double, and triple layers of $[C_4mim]PF_6$ on the graphite surfaces was shown that the mass density profiles of different surface layered films are similar, and the vapor-IL in-

terface appears to have little effect on the layered IL formation. Moreover, it is also shown that the thickness of the monolayer or the bottom layer away from the graphite surface is nearly identical, *i.e.*, 6.0 Å. Very early simulations of a short alkyl chain IL, dimethylimidazolium chloride, have indicated a layered surface with a clear oscillatory density profile akin to that observed for liquid metals [117]. It was also found that $[C_4mim]PF_6$ exhibit density oscillations at the liquid-vapor interface [119-121]. However, the density oscillation of dimethylimidazolium chloride is more obvious than that of $[C_4mim]PF_6$. From MD simulation, vapor-IL interface appears to have little effect on the layered IL formation. In the monolayer, the interaction energy between per cation and per anion is −175.29 kJ/mol. The interaction energy between per ion and the graphite also achieves a comparable quantity of -80.54 kJ/mol. This may be used for the explanation that the strong configurational effect and the interactions between the graphite surface and IL molecules induce the ordering of IL and stretching into a couple of IL layers. Furthermore, the above results imply that the configurational effect and the interactions between the IL layers and the graphite collectively induce different degrees of layered distribution. The vapor-IL interface may disorder to some extent the ordering of the outmost layer and weaken the interactions between the underlayers, resulting in a lower mass density peak of the outmost layer and higher mass density peak of the underlayer. This finding is important for the understanding of modification or lubrication mechanisms of ILs on solid surfaces, especially on the surfaces of carbon nanotubes and carbon black.

The behavior of a model IL, $[C_1mim]Cl$, confined between two parallel walls have been studied at various inter-wall distances, focusing on confinement effects on the structure and dynamics of the ions, and its impact on the charge-transport capacity [164]. The results focus both on structural and dynamical properties. Mass and charge density along the confinement axis reveal a structure of layers parallel to the walls that lead to an oscillatory profile in the electrostatic potential. Orientational correlation functions indicate that cations at the interface orient tilted with respect to the surface and that any other orientational order is lost thereafter. The diffusion coefficients of the ions exhibit a maximum as a function of the confinement distance, a behavior that results from a combination of the structure of the liquid as a whole and a faster molecular motion in the vicinity of the walls. Density profiles perpendicular to the walls confirmed an interfacial liquid layer twice as dense as the bulk followed by oscillations that decay toward the center of the cell; a major part of the layering is due to the distribution of anions. The number of layers changes with the interwall distance and so does the concentration of ions at the interface, showing a maximum at 28 Å. The observed structural effects result from the response of the liquid to the boundary conditions imposed and are detected also in the pressure on the walls. The pressure is determined by the number of particles in the first density layer, a result of the short-range interactions between the atoms and the walls. This effect depends on the details of the ion-wall interactions and may be significantly different in the case of charged surfaces. This is a result that, in light of recent experimental findings [143], may be independent of the type of confining walls used in simulations.

The distribution of charge perpendicular to the surface was determined by the arrangement of the ions and, in particular, by the alignment of the cations. As a result, any test charge entering the liquid encounters a first layer of positive charge followed by a second layer of opposite sign. The electrostatic potential drop between a point inside the walls and the middle of the liquid slab was around -0.5 V, although the potential oscillates strongly into the liquid.

An interesting result is that, under confinement, ionic diffusion is faster than in the bulk, at least in the presence of noncorrugated walls. Ions close to the surfaces diffuse faster than those in the middle of the slab and the diffusion coefficients reflect the changes in the density and proportion of ions near the walls. The reasons for the faster diffusion near the walls may be related to their lack of corrugation, their solvophobic nature, or a combination of both. However, it must also be kept in mind that the local mobility depends on the local density and orientation of the ions, which are the result of collective structural effects.

If the observed trends in ionic mobility apply also to more realistic surfaces, then the higher diffusivity of the ions will surely have an impact on the electrical conductivity and response of the IL to internal electric field changes. In fact, it has been proposed that the ability of the liquid to screen, fast and efficiently, an external field controls the rate of charge-carrier percolation across the nanocrystalline film.

There are several aspects of ILs that need further attention in connection with their uses in solar cells. First, a more realistic modeling of the walls would be necessary as well as the consideration of more sophisticated ILs. Second, it is important to understand the dynamical response of the semiconductor/IL interface to changes in the surface charge.

A recent comprehensive computer simulation of ILs at the SiO_2 surface clearly revealed that the interfacial structure is sensitive to polar or apolar surface as well as hydrophobic or hydrophilic IL components. The study nicely corroborates the experimental sum frequency generation vibrational spectroscopy (SFG) studies of ILs at SiO_2 substrate. Despite the detailed interfacial structure depending on the nature of substrate and ILs, a common feature shared by these simulations is the well-ordered structure at the IL/solid interface. Such ordered interfacial structure was also found in both simulation and experimental SFG study of the IL/TiO_2 interface, as well as the simulations of the IL/graphite interface by Wu *et al.* [163] and by Kislenko *et al.* [165]. Wu's latter study also highlights the solidation of ILs at graphite, as analogue to the confined ILs in carbon nanotube. Recently, Reichert and co-workers [166] investigated ILs interfacial ordering mechanism at the charged Al2O3 substrate via high-energy X-ray reflectivity and observed strong interfacial layering which decays exponentially into the bulk region. Such interfacial layering was expected to be a generic trait of ILs at charged walls. Understanding the interfacial structure, especially the electric double layer (EDL), is crucial in exploring the applications of ILs in electrochemical devices. Recently, Kornyshev [167] proposed a mean-field theory in which a compressibility parameter γ is incorporated. It was shown that the differential capacitance (DC) is bell-shaped when $\gamma > 1/3$, and it is came l-shaped otherwise, while the U-shaped DC, predicted by the classical Couy-Chapman theory, is recovered for the $\gamma > 0$ limit for the infinite dilute electrolyte solution. The bell-shaped DC is supported by Oldham's modification of the Couy-Chapman model for ionic liquid interface in a specific case with $\gamma = 1$. The bell-shaped DC was ob-

served experimentally on an IL/metal electrode (platinum and gold), with similar IL ion sizes, by Ohsaka and co-workers [101]. The study highlights the compressibility of ILs and the different sizes of cations and anions. The focus was on liquid-solid systems and reported molecular dynamics studies at the liquid-solid interface between imidazolium-based ILs, [C_4mim]PF_6 and [C_8mim]PF_6, and an apolar uncharged graphite surface. The main aim of the study was to investigate the influence of different alkyl-side chain lengths of imidazolium on the interfacial structures. The density of IL was much enhanced at the interfacial region and the density oscillation extended to ~15 Å into the bulk with three layers. The results also demonstrated the polar groups tend to aggregate forming a polar network while the nonpolar groups fill up the rest of the vacancy. The imidazolium rings and the side chains preferentially lie flat at the graphite surface with the alkyl side chains of the cations elongated at the interfacial region, and the cations are closer to the graphite surface (ca. 3.6-3.7 Å) than the anions. The surface potential drop across the interface is more profound for [C_8mim]PF_6 than for [C_4mim]PF_6 due to relatively larger local density of the anions for [C_8mim]PF_6 near the graphite surface.

7. Liquid-to-solid phase transition of ionic liquids monolayer confined between graphite walls

While receiving much attention due to ILs importance in a broad range of applications, yet little is understood about their microstructure and phase transition in confined systems. Understanding the microstructure and freezing processes of ILs in confined systems is of practical importance in lubrication, adhesion, and the fabrication of solar cells or IL/nanomaterial composites, in which ILs are in contact with solid surfaces or under confinement. In general, the reduction of the liquid film thickness to fewer than 4-6 molecular layers will promote solidification. This results from the characteristic transverse density profile of thin films, which can induce lateral ordering and lead to freezing. Some evidence has indicated a possible liquid-solid phase transition for ILs in confined systems. Several reports have also revealed the astonishing property of melting point depression of 1,3-dialkylimidazolium-based ILs confined to nanospaces, which was discovered utilizing differential scanning thermal calorimetry. However, the phase behavior of ILs confined to nanospaces remains largely unexplored. The first simulation results of a liquid-solid freezing transition of [C_1mim]Cl IL between two parallel graphite walls has been reported by Sha *et al.* [168]. Their result is of importance to understand the interfacial interactions between ILs and carbon nanotubes because of dispersing uniformly on the surface of single-walled carbon nanotubes via simple mulling. The molecular dynamics simulations were utilized to investigate the freezing of a [C_1mim]Cl monolayer. The simulations predicted a first-order freezing transition from a liquid monolayer to a solid monolayer induced by varying the distance between the parallel graphite walls. The resulting monolayer solid consisting of a hydrogen-bonded network structure is very different from bulk crystalline [C_1mim]Cl. The phase transition can be induced only at a molecular surface density of $\varrho = 1.9/nm^2$. It is important to note that [C_1mim]Cl IL confined between hydrophobic walls indicated no "hardening" or

transition to a solid like phase structure, but only down to a wall distance of 2.5 nm. The wall distance plays a crucial role in the phase transition. Like an ice monolayer confined between walls, the molecule area density ($\varrho = N/l_x l_y$) of [C_1mim]Cl is another important factor. During the simulations, the molecule number of the system was decreased in steps and simulated for time periods equal to the first set of simulations. The change in N reflects the change in surface density since the area of the graphite wall remains unchanged in the simulation. As the molecule number is decreased, the lateral pressure of the monolayer liquid decreases to a lower value. If the surface density exceeds this value, a solid monolayer will not be formed. Meanwhile, the interaction energy between the IL and the walls is about -62 kJ/mol at a distance of 0.7 nm. Hence, the results imply that the configurational effect and the attraction interaction between the IL and the walls collectively induce the solid monolayer. The distance dependences of the diffusion coefficient and the potential energy indicate a strong first-order phase transition in confined [C_1mim]Cl. These results are helpful for the understanding of microstructures of ILs in nanostructured confinement as well as the thermodynamic mechanism of liquid-to-solid phase transition.

For the applications of electrolyte membranes and catalysts, there is a need to immobilize ILs on solid supports or within a solid matrix.

The microstructure of the IL bilayer was studied by varying the graphite wall distance. A liquid-to-solid phase transition of bilayer [C_1mim]Cl was observed at 425 K in this confined system, whereas the melting point of the bulk [C_1mim]Cl crystal is 399 K. Further calculation indicates a high melting point of the confined IL: melting point ~825-850 K. The imidazolium ring of the solid bilayer forms a strong $\pi...\pi$ stacking structure in which each cation is surrounded by the three nearest-neighbor anions. The bilayer solid is a new phase of [C_1mim]Cl differing from the monolayer solid [168] under identical confinement conditions or the bulk crystal.

The simulation on the [C_4mim]NO_3/rutile (110) system shows that the adsorbed NO_3 anions at the interface organized themselves into a highly ordered manner, while changing the anion to PF_6^- does not present such an ordered interfacial structure. On the other hand, Grimes and co-workers have conducted experiments to study the high rate photocatalytic conversion of CO_2 to hydrocarbon production on the high surface area TiO_2 nanotube arrays.

An operating efficiency of electrochemical devices is greatly influenced by the molecular structure of the electrode/electrolyte interface. For example, the electron lifetime and open-circuit voltage in dye-sensitized solar cells depend on the structure of the electrical double layer (EDL). The specific capacitance of supercapacitors also depends on the EDL structure and is capable of being varied on change of the ions or even molecular ion fragments in IL. However, a double layer in ILs has not yet been adequately explored.

8. The structure of ionic liquid [C_4mim]PF_6/rutile (110) interface

The dye-sensitized solar cells (DSSCs) have been extensively investigated since their applications in the production of high light-to-electricity conversion efficiency. Traditionally, the devi-

ces are immersed in electrolytes, which are usually composed of an I$^-$/I$_3^-$ redox couple and organic solvents such as acetonitrile. IL crystal system (C$_{12}$mim$^+$/I$^-$/I$_2$) has been used as electrolyte of dye-sensitized TiO$_2$ solar cells; it has been found that though large viscosity of the IL, the diffusion coefficient is still high since the exchange reactions facilitate the charge transport process. To acquire detailed information of DSSCs, Aliaga and Baldelli have performed a sum frequency generation study on one component of the solar devices, the liquid/solid interface between [C$_4$mim]DCA and [C$_4$mim]MS and TiO$_2$. The results pointed out that both the ions are present at the interface for [C$_4$mim]DCA while only the cations are detected for [C$_4$mim]MS. The spectra also emphasized on a stronger charge adsorption of the DCA anions than the MS anions. In addition to experimental researches, it has been previously shown that the interface between [C$_4$mim]NO$_3$ and rutile (110) surface by means of molecular dynamics simulation. The results indicated that the NO$_3$ anions prefer to aggregate at the interface and arrange themselves in a highly ordered manner. As for the [C$_4$mim]$^+$ cations, occupying the region adjacent to the NO$_3^-$ layer, they tend to stand vertically on the TiO$_2$ (110) surface.

Shu *et al.* [169] presented a simulation on the interface between [C$_4$mim]PF$_6$ and rutile TiO$_2$ (110) surface, considering the other polymorphs of TiO$_2$ are less stable at room temperature. The main objective of their work was to model the IL/semiconductor interface, where the recombination process occurs, and study the structural behaviors of the confined IL. The results revealed that both ions are gathered on the surface, forming ionic double layers with regularity. It is also interesting to see that the cations lie flat on the surface, with alkyls stretched out in the bottom region. In addition, the ions are assembled at the interface, forming several enhanced layers at each side of the slab and are self-organized into alternate double ionic layers. The adsorbed cations are inclined to lie flat on the rutile (110) surface-This MD simulation casts new light on the microscopic structure features on the IL/solid interface and provides insights on the development of DSSCs. They have performed a molecular dynamics simulation on the [C$_4$mim]PF$_6$/ rutile (110) system.

Thanks to their low vapor pressure, ILs are ideal extraction solvents or reaction media because simple evaporation methods can be used to separate solutes from ILs. In addition, ILs can be custom-made with targeted functions. Because of these advantages, ionic liquids have been engineered as extraction solvents, reaction media and drug delivery materials. In most IL applications – such as extraction, lubrication, and IL super capacitors – the core function of the IL occurs at the ionic liquid–solid interfaces. Ionic liquids are different from conventional molecular liquids because no individual molecule exists in the liquid. Moreover, they are not diluted electrolyte solutions either. Hence, no existing theory and model can precisely describe the behavior of ILs, especially at the IL interfaces. Therefore, studies of the IL interfacial properties are necessary for further developments of IL-based applications. Furthermore, new applications – such as IL reactor, IL-circuit, and surface pattern visualization – require the precise control over the position of the IL drop on surface. The chemical pattern-directed assembly of IL on surface has been under investigation by Zhang *et al.* [170]. The chemical patterns can control the shape, size, and position of the IL on surface. Furthermore, IL drops on surface can be coated with a layer of silane film, forming an IL capsule.

However, experimental data are still lack, and none of the existing theories can completely explain the much diversity. Thus, first, the challenge for surface chemists, electrochemists, and theoreticians is to understand the detailed interface structure, including the adsorption, configuration, distribution, and orientation of ILs on the electrode surface. Some new models, new experimental techniques, and the details of this important system should be explored in the future to further realize the IL/electrode interface structures. Moreover, up to now, only quite a few number of ILs species were studied as models. However, the interface properties, structure and functions of the ILs with different cations and anions on the electrodes varies distinguishably. Thus, there is a need to have systematic studies on a wide range of ionic liquids so that more meaningful and comparable results can be obtained.

In an IL system, the heterogeneous electron transfer kinetics is highly dependent on the nature of both cation and anion in ILs. In addition, it should be pointed out that the physicochemical properties of ILs are largely dependent on the temperature and impurities such as water and some organic solvents, which will remarkably affect the transport and heterogeneous electron transfer ability. Though vast works have been carried out in this aspect, there is a huge data gap with respect to the thermodynamic and transport properties over a wide range of temperatures, as well as the effect of solutes and impurities on these properties. It is worth noting that the classical Marcus theory for outer sphere electron transfer, which is based on the reorganization of solvent dipoles, is not suitable to the entire ion systems of ILs. Developing a novel theory and electron transfer model system for the entire ion systems to explain the electron transfer process in ILs is also an important task in the future.

To date, the applications of ILs have involved nearly all aspects of electrochemistry, such as electrodeposition, electrosynthesis, electrochemical capacitors, electrochemical biosensors, and lithium batteries. Besides those stated above, it was recently shown that ILs can be used as a simple and effective way to reduce the scattering of carriers by charged impurities in graphene transistors supported on solid substrates [171].

Confinement can induce unusual behavior in the properties of matter. Using molecular dynamics simulations, a liquid-to-solid transition of a bilayer of $[C_1mim]Cl$ confined between graphite walls was studied in order to mimic the phase transition of an IL confined to hydrophobic nanospace. It was found that the IL bilayer undergoes a clear and drastic phase transition at a wall distance of about 1.1 nm, forming a new high-melting-point solid phase with different hydrogen bonding networks. In the new phase, each cation is surrounded by the three nearestneighbor anions, and each anion is also encircled by the three nearest-neighbor cations. Strong π-π stacking interactions are found between the cations of the bilayer solid. The anions can be formed into a hexagonal ring around the cations. The new bilayer solid is a high-melting-point crystal possessing a melting point of 825-850 K, which is higher than that of the bulk crystal by more than 400 K.

For imidazolium-based ILs, the effect of the alkyl-chain length on the differential capacitance of EDL, electrocapillary curves, and the potential of zero charge (PZC) were experimentally investigated [8,9]. Based on the results obtained, a qualitative pattern of the $Hg/[C_8mim]BF_4$ interface at the electrode potentials close to PZC was suggested [9]. A quantitative information on the EDL structure is given in a number of papers wherein the imidazolium cations' orientation at

the platinum and quartz surfaces has been determined using the sum frequency generation vibrational spectroscopy [10–13]. Since the electrode/electrolyte interface affects appreciably the relevant electrochemical processes, the development of adequate theoretical models of EDL in ILs takes on great significance. Owing to high ion concentration in ILs, the Gouy-Chapman classical theory is no longer valid and the double layer model must take into account a finite size of ions [14]. Investigating the double layer in IL $[C_4mim]PF_6$ at the graphite surface by use of the molecular dynamics simulation was the major goal for Kislenko, Samoylov, and Amirov [165].

Account was also taken of a large body of experimental and theoretical data available for comparison with the simulation results. The basal plane of graphite emulates the surface of an activated carbon used as an electrode material for supercapacitors. The calculations were performed both for an uncharged graphite surface and for positively and negatively charged ones. It is found that near an uncharged surface the IL structure differs from its bulk structure and represents a well-ordered region, extending over 20 Å from the surface. Three dense layers of ca 5 Å thick are clearly observed at the interface, composed of negative ions and positively charged rings. It is established that in the first adsorption layer the imidazolium ring in the $[C_4mim]^+$ cation tends to be arranged in parallel to the graphite surface at a distance of 3.5 Å. The PF_6^- anion is oriented in such a way that the phosphorus atom is at a distance of 4.1 Å from the surface and triplets of fluorine atoms form two planes parallel to the graphite surface. Ions adsorbed at the uncharged surface are arranged in a highly defective 2D hexagonal lattice and the corresponding lattice spacing is approximately four times larger than that of the graphene substrate. The influence of the electrode potential on the distribution of electrolyte ions and their orientation has also been investigated. Increase in the electrode potential induces broadening of the angle distribution of adsorbed rings and a shift of the most probable tilt angle towards bigger values. It was shown that there are no adsorbed anions on the negatively charged surface, but the surface concentration of adsorbed cations on the positively charged surface has a non-zero value. In addition, the influence of the surface charge on the volume charge density and electric potential profiles in an electrolyte was studied. The differences in the cation and anion structure result in the fact that the integral capacitance of the electrical double layer depends on the electrode polarity. The phenomena confirmed experimentally such interfacial layers formation and increase of an average tilt angle of adsorbed rings with increasing the electrode potential. In addition, the calculated values of the EDL capacitance coincide in the order of magnitude with the experimentally measured specific capacitance at the electrode/IL interface for activated carbons as electrode material and imidazolium-based ILs.

Author details

Fatemeh Moosavi

Address all correspondence to: moosavibaigi@um.ac.ir

Department of Chemistry, Ferdowsi University of Mashhad, Mashhad, Iran

References

[1] Patil ML, Rao CVL, Yonezawa K, Takizawa S, Onitsuka K, Sasai H. Design and Synthesis of Novel Chiral Spiro Ionic Liquids. Organic Letters 2006; 8(2) 227–230.

[2] Newington I, Perez-Arlandis JM, Welton T. Ionic Liquids as Designer Solvents for Nucleophilic Aromatic Substitutions. Organic Letters 2007; 9(25) 5247–5250.

[3] Gale RJ, Osteryoung RA. Electrochemical Reduction of Pyridinium Ions in ionic Aluminum Chloride: Alkylpyridinium Halide Ambient Temperature Liquids. Journal of the Electrochemical Society 1980; 127(10) 2167–2172.

[4] Wilkes JS, Levisky JA, Wilson RA, Hussey CL. Dialkylimidazolium Chloroaluminate Melts: A New Class of Room-Temperature Ionic Liquids for Electrochemistry, Spectroscopy and Synthesis. Inorganic Chemistry 1982; 21(3), 1263–1264.

[5] Fung YS, Zhu DR. Electrodeposited Tin Coating as Negative Electrode Material for Lithium-Ion Battery in Room Temperature Molten Salt. Journal of the Electrochemical Society 2002; 149(3) A319–A324.

[6] Shobukawa H, Tokuda H, Susan MABH, Watanabe M. Ion Transport Properties of Lithium Ionic Liquids and Their Ion Gels. Electrochimica Acta 2005; 50(19) 3872–3877.

[7] Shobukawa H, Tokuda H, Tabata SI, Watanabe M. Preparation and Transport Properties of Novel Lithium Ionic Liquids. Electrochimica Acta 2004; 50(2-3) 305–309.

[8] Seki S, Kobayashi Y, Miyashiro H, Ohno Y, Usami A, Mita Y, Watanabe M, Terada N. Highly Reversible Lithium Metal Secondary Battery Using a Room Temperature Ionic Liquid/Lithium Salt Mixture and a Surface-Coated Cathode Active Material. Chemical Communications 2006; (5) 544–545.

[9] Stenger-Smith JD, Webber CK, Anderson N, Chafin AP, Zong K, Reynolds JR. Poly(3,4-alkylenedioxythiophene)-Based Supercapacitors Using Ionic Liquids as Supporting Electrolytes. Journal of the Electrochemical Society 2002; 149(8) A973–A977.

[10] Sato T, Masuda G, Takagi K. Electrochemical Properties of Novel Ionic Liquids for Electric Double Layer Capacitor Applications. Electrochimica Acta 2004; 49(21) 3603–3611.

[11] Liu H, He P, Li Z, Liu Y, Li J. A Novel Nickel-Based Mixed Rare-Earth Oxide/Activated Carbon Supercapacitor Using Room Temperature Ionic Liquid Electrolyte, Electrochimica Acta, 2006; 51(10) 1925–1931.

[12] Noda A, Susan MABH, Kudo K, Mitsushima S, Hayamizu K, Watanabe M. Brønsted Acid-Base Ionic Liquids as Proton-Conducting Nonaqueous Electrolytes. Journal of Physical Chemistry B 2003; 107(17) 4024–4033.

[13] Kubo W, Murakoshi K, Kitamura T, Quasi-Solid-State Dye-Sensitized TiO_2 Solar Cells: Effective Charge Transport in Mesoporous Space Filled with Gel Electrolytes

Containing Iodide and Iodine. Journal of Physical Chemistry B 2001; 105(51) 12809–12815.

[14] Kubo W, Kitamura T, Hanabusa K, Wada Y, Yanagida S. Quasi-Solid-State Dye-Sensitized Solar Cells using Room Temperature Molten Salts and a Low Molecular Weight Gelator. Chemical Communications 2002; (4) 374–375.

[15] Wang P, Zakeeruddin SM, Moser JE, Grätzel M. A New Ionic Liquid Electrolyte Enhances the Conversion Efficiency of Dye-Sensitized Solar Cells. Journal of Physical Chemistry B 2003; 107(48) 13280–13285.

[16] Xia J, Masaki N, Jiang K, Yanagida S. Deposition of a Thin Film of TiO_x from a Titanium Metal Target as Novel Blocking Layers at Conducting Glass/TiO_2 Interfaces in Ionic Liquid Mesoscopic TiO_2 Dye-Sensitized Solar Cells. Journal of Physical Chemistry B 2006; 110(50) 25222–25228.

[17] Wang P, Zakeeruddin SM, Moser JE, Humphry-Baker R, Grätzel M. A Solvent-Free, $SeCN^-/(SeCN)_3^-$ Based Ionic Liquid Electrolyte for High-Efficiency Dye-Sensitized Nanocrystalline Solar Cells. Journal of the American Chemical Society 2004; 126(23) 7164–7165.

[18] Wang P, Zakeeruddin SM, Comte P, Exnar I, Grätzel M. Gelation of Ionic Liquid-Based Electrolytes with Silica Nanoparticles for Quasi-Solid-State Dye-Sensitized Solar Cells. Journal of the American Chemical Society 2003; 125(5) 1166–1167.

[19] Zhou D, Spinks GM, Wallace GG, Tiyapiboonchaiya C, MacFarlane DR, Forsyth M, Sun J. Solid State Actuators Based on Polypyrrole and Polymer-in-Ionic Liquid Electrolytes. Electrochimica Acta, 2003; 48(14–16) 2355–2359.

[20] Anderson JL, Armstrong DW. High-Stability Ionic Liquids. A New Class of Stationary Phases for Gas Chromatography. Analytical Chemistry 2003; 75(18) 4851–4858.

[21] Xiaohua X, Liang Z, Xia L, Shengxiang J. Ionic Liquids as Additives in High Performance Liquid Chromatography: Analysis of Amines and the Interaction Mechanism of Ionic Liquids. Analytica Chimica Acta 2004; 519(2) 207–211.

[22] Peng JF, Liu JF, Hu XL, Jiang GB. Direct Determination of Chlorophenols in Environmental Water Samples by Hollow Fiber Supported Ionic Liquid Membrane Extraction Coupled with High-Performance Liquid Chromatography. Journal of Chromatography A 2007; 1139(2) 165–170.

[23] Qi S, Cui S, Cheng Y, Chen X, Hu Z. Rapid Separation and Determination of Aconitine Alkaloids in Traditional Chinese Herbs by Capillary Electrophoresis using 1-Butyl-3-Methylimidazoium-Based Ionic Liquid as Running Electrolyte. Biomedical Chromatography 2006; 20(3) 294–300.

[24] Tian K, Qi S, Cheng Y, Chen X, Hu Z. Separation and Determination of Lignans from Seeds of Schisandra Species by Micellar Electrokinetic Capillary Chromatography using Ionic Liquid as Modifier. Journal of Chromatography A 2005; 1078(1-2) 181–187.

[25] Oter O, Ertekin K, Topkaya D, Alp S. Room Temperature Ionic Liquids as Optical Sensor Matrix Materials for Gaseous and Dissolved CO_2. Sensors and Actuators B: Chemical 2006; 117(1) 295–301.

[26] Fletcher KA, Pandey S, Storey IK, Hendricks AE, Pandey S. Selective Fluorescence Quenching of Polycyclic Aromatic Hydrocarbons by Nitromethane within Room Temperature Ionic Liquid 1-Butyl-3-Methylimidazolium Hexafluorophosphate. Analytica Chimica Acta 2002; 453(1) 89–96.

[27] Mank M, Stahl B, Boehm G. 2,5-Dihydroxybenzoic Acid Butylamine and other Ionic Liquid Matrixes for Enhanced MALDI-MS Analysis of Biomolecules. Analytical Chemistry 2004; 76(10) 2938–2950.

[28] Welton T. Room Temperature Ionic Liquids. Solvents for Synthesis and Catalysis. Chemical Reviews 1999; 99(8) 2071–2083.

[29] Wasserscheid P, Keim W. Ionic Liquids-New "Solutions" for Transition Metal Catalysis. Angewandte Chemie International Edition 2000; 39(21) 3772–3789.

[30] Huddleston JG, Visser AE, Reichert WM, Willauer HD, Broke GA, Rogers RD. Characterization and Comparison of Hydrophilic and Hydrophobic Room Temperature Ionic Liquids Incorporating the Imidazolium Cation. Green Chemistry 2001; 3(4) 156–164.

[31] Dupont J, de Souza RF, Suarez PAZ, Ionic Liquid (Molten Salt) Phase Organometallic Catalysis, Chemical Reviews 2002; 102(10) 3667–3692.

[32] Wasserscheid P, Welton T. Ionic Liquids in Synthesis, John Wiley & Sons: New York; 2002.

[33] Welton T. Ionic liquids in Catalysis. Coordination Chemistry Reviews 2004; 248(21-24) 2459–2477.

[34] Buzzeo MC, Evans RG, Compton RG. Non-Haloaluminate Room-Temperature Ionic Liquids in Electrochemistry. ChemPhysChem 2004; 5(8) 1106–1120.

[35] Baker GA, Baker SN, Pandey S, Bright FV. An Analytical View of Ionic Liquids. Analyst 2005; 130(6) 800–808.

[36] Weyershausen B, Lehmann K. Industrial Application of Ionic Liquids as Performance Additives, Green Chemistry 2005; 7(1) 15–19.

[37] Zhang S, Sun N, He X, Lu X, Zhang X. Physical Properties of Ionic Liquids: Database and Evaluation. Journal of Physical and Chemical Reference Data 2006; 35(4) 1475–1517.

[38] Anderson JL, Armstrong DW, Wei GT. Ionic Liquids in Analytical Chemistry. Analytical Chemistry 2006; 78(9) 2892–2902.

[39] Galiński M, Lewandowski A, Stępniak I. Ionic liquids as Electrolytes. Electrochimica Acta 2006; 51(26) 5567–5580.

[40] Pârvulescu VI, Hardacre C. Catalysis in Ionic Liquids. Chemical Review 2007; 107(6) 2615–2665.

[41] Greaves TL, Drummond CJ. Ionic liquids as Amphiphile Self-Assembly Media. Chemical Society Reviews 2008; 37(8) 1709–1726.

[42] Hapiot P, Lagrost C. Electrochemical Reactivity in Room-Temperature Ionic Liquids. Chemical Review 2008; 108(7) 2238–2264.

[43] Greaves TL, Drummond CJ. Protic Ionic Liquids: Properties and Applications, Chemical Review 2008; 108(1) 206–237.

[44] Armand M, Endres F, MacFarlane DR, Ohno H, Scrosati B. Ionic-Liquid Materials for the Electrochemical Challenges of the Future. Nature Materials 2009; 8(6) 621–629.

[45] Singh VV, Nigam AK, Batra A, Boopathi M, Singh B, Vijayaraghavan R. Applications of Ionic Liquids in Electrochemical Sensors and Biosensors. International Journal of Electrochemistry 2012; 2012, Article ID 165683, 19 pages.

[46] Fuller J, Carlin RT, Osteryoung RA. The Room Temperature Ionic Liquid 1-Ethyl-3-Methylimidazolium Tetrafluoroborate: Electrochemical Couples and Physical Properties. Journal of the Electrochemical Society 1997; 144(11) 3881–3886.

[47] Quinn BM, Ding Z, Moulton R, Bard AJ. Novel Electrochemical Studies of Ionic Liquids. Langmuir 2002; 18(5) 1734–1742.

[48] Holbrey JD, Seddon KR, Ionic liquids. Clean Products and Processes 1999; 1(4) 223–236.

[49] Trulove PC, Mantz RA. Electrochemical Properties of Ionic Liquids, in Ionic Liquids in Synthesis, Welton T, Wasserscheld P. Eds., p. 368, John Wiley & Sons, Morlenbach, Germany, 2003.

[50] Conway BE. Electrochemical Supercapacitors: Scientific Fundamentals and Technological Applications; Kluwer Academics and Plenum: New York, 1999.

[51] Simon P, Gogotsi Y. Materials for Electrochemical Capacitors. Nature Materials 2008; 7(11) 845–854.

[52] Miller JR, Simon P. Electrochemical Capacitors for Energy Management. Science 2008; 321(5889) 651–652.

[53] McEwen AB, McDevitt SF, Koch VR, Nonaqueous Electrolytes for Electrochemical Capacitors: Imidazolium Cations and Inorganic Fluorides with Organic Carbonates, Journal of the Electrochemical Society 1997; 144(4) L84–L86; McEwen AB, Ngo HL, LeCompte K, Goldman JL. Electrochemical Properties of Imidazolium Salt Electrolytes for Electrochemical Capacitor Applications, Journal of the Electrochemical Society 1999; 146(5) 1687–1695.

[54] Katakabe T, Kaneko T, Watanabe M, Fukushima T, Aida T. Electric Double-Layer Ca‐
pacitors Using "Bucky Gels" Consisting of an Ionic Liquid and Carbon Nanotubes.
Journal of the Electrochemical Society 2005; 152(10) A1913–A1916.

[55] Laforgue A, Simon P, Fauvarque JF, Mastragostino M, Soavi F, Sarrau JF, Lailler P,
Conte M, Rossi E, Saguatti S. Activated Carbon/Conducting Polymer Hybrid Super‐
capacitors BATTERIES AND ENERGY CONVERSION. Journal of the Electrochemi‐
cal Society 2003; 150(5) A645–A651.

[56] Balducci A, Henderson WA, Mastragostino M, Passerini S, Simon P, Soavi F. Cycling
Stability of a Hybrid Activated Carbon//Poly(3-Methylthiophene) Supercapacitor
with N-Butyl-N-Methylpyrrolidinium Bis(Trifluoromethanesulfonyl)Imide Ionic Liq‐
uid as Electrolyte. Electrochimica Acta 2005; 50(11) 2233–2237.

[57] Potts JR, Dreyer DR, Bielawski CW, Ruoff RS. Graphene-Based Polymer Nanocom‐
posites. Polymer 2011; 52(1) 5–25.

[58] Geim AK, Novoselov KS. The Rise of Graphene. Nature Materials 2007; 6(3) 183–191.

[59] Novoselov KS, Geim AK, Morozov SV, Jiang D, Zhang Y, Dubonos SV, Grigorieva
IV, Firsov AA. Electric Field Effect in Atomically Thin Carbon Films. Science 2004;
306(5696) 666–669.

[60] Stoller MD, Park S, Zhu Y, An J, Ruoff RS. Graphene-Based Ultracapacitors. Nano
Letters 2008; 8(10) 3498–3502.

[61] Wang Y, Shi Z, Huang Y, Ma Y, Wang C, Chen M, Chen Y. Supercapacitor Devices
Based on Graphene Materials. Journal of Physical Chemistry C 2009; 113(30) 13103–
13107.

[62] Stankovich S, Dikin DA, Dommett GHB, Kohlhaas KM, Zimney EJ, Stach EA, Piner
RD, Nguyen ST, Ruoff RS. Graphene-Based Composite Materials. Nature 2006;
442(7100) 282–286.

[63] Kötz R, Carlen M. Principles and Applications of Electrochemical Capacitors. Electro‐
chimica Acta 2000; 45(15-16) 2483–2498.

[64] Islam MM, Alam MT, Okajima T, Ohsaka T. Electrical Double Layer Structure in Ion‐
ic Liquids: An Understanding of the Unusual Capacitance–Potential Curve at a Non‐
metallic Electrode. Journal of Physical Chemistry C 2009; 113(9) 3386–3389.

[65] Largeot C, Portet C, Chmiola J, Taberna P, Gogotsi Y, Simon P. Relation between the
Ion Size and Pore Size for an Electric Double–Layer Capacitor. Journal of the Ameri‐
can Chemical Society 2008; 130(9) 2730–2731.

[66] Kim T, Lee H, Kim J, Suh KS. Synthesis of Phase Transferable Graphene Sheets Using
Ionic Liquid Polymers. ACS Nano 2010; 4(3) 1612–1618.

[67] Webber A, Blomgren GE. Ionic Liquids for Lithium Ion and Related Batteries, in Ad‐
vances in Lithium-Ion Batteries, W. A. van Schalkwijk and B. Scrosati, Editors, p. 185,

Kluwer Academic / Plenum Publishers, New York (2002); Wilkes JS. The Past, Present and Future of Ionic Liquids as Battery Electrolytes, in Green Industrial Applications of Ionic Liquids, Rogers RD, Seddon KR, Volkov S. Editors, p. 295, NATO Science Series, Vol. 92, Kluwer Academic Publishers, Dordrecht, The Netherlands (2002).

[68]   Caja J, Dunstan TDJ, Ryan DM, Katovic V, in Molten Salts XII, P. C. Trulove, H. C. De Long, G. R. Stafford, and S. Deki, Editors, PV 99-41, p. 150, The Electrochemical Society Proceedings Series, Pennington, NJ (1999).

[69]   Matsumoto H, Sakaebe H, Tatsumi K, Kikuta M, Ishiko E, Kono M. Fast Cycling of Li/LiCoO$_2$ Cell with Low-Viscosity Ionic Liquids Based on Bis(Fluorosulfonyl)Imide [FSI]. Journal of Power Sources 2006; 160(2) 1308–1313.

[70]   Ishikawa M, Sugimoto T, Kikuta M, Ishiko E, Kono M. Pure Ionic Liquid Electrolytes Compatible with a Graphitized Carbon Negative Electrode in Rechargeable Lithium-Ion Batteries. Journal of Power Sources 2006; 162(1) 658–662.

[71]   Garcia B, Lavallee S, Perron G, Michot C, Armand M. Room Temperature Molten Salts As Lithium Battery Electrolyte, Electrochimica Acta 2004; 49(26) 4583–4588.

[72]   Howlett PC, Brack N, Hollenkamp AF, Forsyth M, MacFarlane DR. Characterization of the Lithium Surface in N-Methyl-N-alkylpyrrolidinium Bis(trifluoromethanesulfonyl)amide Room-Temperature Ionic Liquid Electrolytes Batteries, Fuel Cells, and Energy Conversion. Journal of Electrochemical Society 2006; 153(3) A595–A606.

[73]   de Andrade J, Boes ES, Stassen H. Computational Study of Room Temperature Molten Salts Composed by 1-Alkyl-3-methylimidazolium Cations-Force-Field Proposal and Validation. Journal of Physical Chemistry B 2002; 106(51), 13344–13351.

[74]   Gale RJ, Osteryoung RA. The Electrical Double Layer at Mercury in Room Temperature Aluminum Chloride: 1-Butylpyridinium Chloride Ionic Liquids. Electrochimica Acta 1980; 25(11) 1527–1529.

[75]   Nanjundiah C, Mcdevitt SF, Koch VR. Differential Capacitance Measurements in Solvent-Free Ionic Liquids at Hg and C Interfaces. Journal of Electrochemical Society 1997; 144(10) 3392–3397.

[76]   Liu H, He P, Li Z, Liu Y, Li J, Zheng L, Li J. The Inherent Capacitive Behavior of Imidazolium-based Room-Temperature Ionic Liquids at Carbon Paste Electrode. Electrochemical and Solid-State Letters 2005; 8(7) J17–J19.

[77]   Lazzari M, Mastragostino M, Soavi F. Capacitance Response of Carbons in Solvent-Free Ionic Liquid Electrolytes. Electrochemistry Communications 2007; 9(7) 1567–1572.

[78]   Alam MT, Islam MM, Okajima T, Ohsaka T. Measurements of Differential Capacitance in Room Temperature Ionic Liquid at Mercury, Glassy Carbon and Gold Electrode Interfaces. Electrochemistry Communications 2007; 9(9) 2370–2374.

[79] Xia J, Chen F, Li J, Tao N. Measurement of the quantum capacitance of graphene, Nature Nanotechnology 2009; 4(8) 505–509.

[80] Crowhurst L, Lancaster NL, Arlandis JMP, Welton T. Manipulating Solute Nucleophilicity with Room Temperature Ionic Liquids. Journal of the American Chemical Society 2004; 126(37) 11549–11555.

[81] Wishart JF, Castner EWJ. The Physical Chemistry of Ionic Liquids. Journal of Physical Chemistry B 2007; 111(18) 4639–4640.

[82] Seddon KR, Ionic Liquids for Clean Technology. Journal of Chemical Technology & Biotechnology 1997; 68(4) 351–356.

[83] Triolo A, Russina O, Bleif HJ, Di Cola E. Nanoscale Segregation in Room Temperature Ionic Liquids. Journal of Physical Chemistry B 2007; 111(18) 4641–4644.

[84] Triolo A, Russina O, Fazio B, Triolo R, Di Cola E. Morphology of 1-Alkyl-3-Methylimidazolium Hexafluorophosphate Room Temperature Ionic Liquids. Chemical Physics Letters 2008; 457(4-6) 362–365.

[85] Xiao D, Rajian JR, Hines LG, Li JS, Bartsch RA, Quitevis EL. Nanostructural Organization and Anion Effects in the Optical Kerr Effect Spectra of Binary Ionic Liquid Mixtures. Journal of Physical Chemistry B 2008; 112(42) 13316–13325.

[86] Bhargava BL, Balasubramanian S, Klein ML. Modelling Room Temperature Ionic Liquids. Chemical Communications 2008; (29) 3339–3351.

[87] Atkin R, Warr GG. The Smallest Amphiphiles: Nanostructure in Protic Room-Temperature Ionic Liquids with Short Alkyl Groups. Journal of Physical Chemistry B 2008; 112(14) 4164–4166.

[88] Horn RG, Evans DF, Ninham BW. Double-Layer and Solvation Forces Measured in a Molten Salt and its Mixtures with Water. Journal of Physical Chemistry 1988; 92 (12) 3531–3537.

[89] Atkin R, Warr GG. Structure in Confined Room-Temperature Ionic Liquids. Journal of Physical Chemistry C 2007; 111(13) 5162–5168.

[90] Wakeham D, Hayes R, Warr GG, Atkin R. Influence of Temperature and Molecular Structure on Ionic Liquid Solvation Layers. Journal of Physical Chemistry B 2009; 113(17) 5961–5966.

[91] Atkin R, Abedin SZE, Hayes R, Gasparotto LHS, Borisenko N, Endres F. AFM and STM Studies on the Surface Interaction of [BMP]TFSA and [EMIm]TFSA Ionic Liquids with Au(111). Journal of Physical Chemistry C 2009; 113(30) 13266–13272.

[92] Hayes R, Abedin SZE, Atkin R. Pronounced Structure in Confined Aprotic Room-Temperature Ionic Liquids. Journal of Physical Chemistry B 2009; 113(20) 7049–7052.

[93] Baldelli S. Probing Electric Fields at the Ionic Liquid–Electrode Interface Using Sum Frequency Generation Spectroscopy and Electrochemistry. Journal of Physical Chemistry B 2005; 109(27) 13049–13051.

[94] Baldelli S. Surface Structure at the Ionic Liquid-Electrified Metal Interface. Accounts of Chemical Research 2008; 41(3) 421–431.

[95] Reed SK, Lanning OJ, Madden PA. Electrochemical Interface Between an Ionic Liquid and a Model Metallic Electrode. The Journal of Chemical Physics 2007; 126(8) 084704(1–13).

[96] Feng G, Zhang JS, Qiao R. Microstructure and Capacitance of the Electrical Double Layers at the Interface of Ionic Liquids and Planar Electrodes. Journal of Physical Chemistry C 2009; 113(11) 4549–4559.

[97] Su YZ, Fu YC, Yan JW, Chen ZB, Mao BW. Double Layer of Au(100)/Ionic Liquid Interface and Its Stability in Imidazolium-Based Ionic Liquids. Angewandte Chemie International Edition 2009; 48(28) 5148–5151.

[98] Fedorov MV, Kornyshev AA. Ionic Liquid near a Charged Wall: Structure and Capacitance of Electrical Double Layer. Journal of Physical Chemistry B 2008; 112(38) 11868–11872.

[99] Fedorov MV, Kornyshev AA. Towards understanding the structure and capacitance of electrical double layer in ionic liquids. Electrochimica Acta 2008; 53(23) 6835–6840.

[100] Oldham KB. A Gouy-Chapman-Stern Model of the Double Layer at a (Metal)/(Ionic Liquid) Interface. Journal of Electroanalytical Chemistry 2008; 613(2) 131–138.

[101] Islam MM, Alam MT, Ohsaka T. Electrical Double-Layer Structure in Ionic Liquids: A Corroboration of the Theoretical Model by Experimental Results. Journal of Physical Chemistry C 2008; 112(42) 16568–16574.

[102] Tsuda T, Hussey CL. Electrochemical Applications of Room-Temperature Ionic Liquids. he Electrochemical Society Interface 2007; 16(1) 42–49.

[103] Wei D, Ivaska A. Applications of Ionic Liquids in Electrochemical Sensors, Analytica Chimica Acta 2008; 607(2) 126–135.

[104] Shvedene NV, Chernyshov DV, Pletnev IV. Ionic liquids in Electrochemical Sensors. Russian Journal of General Chemistry 2008; 78(12) 2507–2520.

[105] Gomes SASS, Nogueira JMF, Rebelo MJF. An Amperometric Biosensor for Polyphenolic Compounds in Red Wine. Biosensors and Bioelectronics 2004; 20(6) 1211–1216.

[106] Liu Y, Shi L, Wang M, Li Z, Liu H, Li J. A Novel Room Temperature Ionic Liquid Sol–Gel Matrix for Amperometric Biosensor Application. Green Chemistry 2005; 7(9) 655–658.

[107] Guo C, Song Y, Wei H, Li P, Wang L, Sun L, Sun Y, Li Z. Room Temperature Ionic Liquid Doped DNA Network Immobilized Horseradish Peroxidase Biosensor for

Amperometric Determination of Hydrogen Peroxide. Analytical and Bioanalytical Chemistry 2007; 389(2) 527–532.

[108] Forzani ES, Lu DL, Leright M, Aguilar AD, Tsow F, Iglesias R, Zhang Q, Lu J, Li JH, Tao NJ. A Hybrid Electrochemical–Colorimetric Sensing Platform for Detection of Explosives, Journal of the American Chemical Society 2009; 131(4) 1390–1391.

[109] Lux SF, Schmuck M, Appetecchi GB, Passerini S, Winter M, Balducci A. Lithium In‐sertion in Graphite from Ternary Ionic Liquid - Lithium Salt Electrolyte. II. Specific Capacity, Cycling Stability and Cycling Efficiency. Journal of Power Sources 2009; 192(2) 606–661.

[110] Liu H, Liu Y, Li J. Ionic Liquids in Surface Electrochemistry. Physical Chemistry Chemical Physics 2010; 12(8) 1685–1697.

[111] Norouzi P, Ganjali MR, Faridbod F, Shahtaheri SJ, Zamani HA. Electrochemical Anion Sensor for Monohydrogen Phosphate Based on Nano-composite Carbon Paste. International Journal of Electrochemical Science 2012; 7(3) 2633–2642.

[112] Sheldon R. Catalytic Reactions in Ionic Liquids. Chemical Communications 2001; (23) 2399–2407.

[113] Huddleston JG, Rogers RD. Room Temperature Ionic Liquids as Novel Media for 'Clean' Liquid–Liquid Extraction. Chemical Communications 1998; (16) 1765–1766.

[114] Abraham MH, Zissimos AM, Huddleson JG, Willauer HD, Rogers RD, Acree WE. Some Novel Liquid Partitioning System: Water-Ionic Liquids and Aqueous Biphasic Systems. Industrial and Engineering Chemistry Research 2003; 42(3) 413–418.

[115] Papageorgiou N, Athanassov Y, Armand M, Bonhote P, Petterson H, Azam A, Grät‐zel M. The Performance and Stability of Ambient Temperature Molten Salts for Solar Cell Applications. Journal of Electrochemical Society 1996; 143(10) 3099–3108.

[116] Nainaparampil JJ, Phillips BS, Eapen KC, Zabinski JS. Micro–nano Behaviour of DMBI-PF$_6$ Ionic Liquid Nanocrystals: Large and Small-Scale Interfaces. Nanotechnol‐ogy 2005; 16(11) 2474–2481.

[117] Mezger M, Schramm S, Schröder H, Reichert H, Deutsch M, De Souza EJ, Okasinski JS, Ocko BM, Honkimäki V, Dosch H. Layering of [BMIM]+-Based Ionic Liquids at a Charged Sapphire Interface. The Journal of Chemical Physics 2009; 131(9) 094701 (1–13).

[118] Lynden-Bell RM. Gas-Liquid Interfaces of Room Temperature Ionic Liquids, Molecu‐lar Physics 2003; 101(16) 2625–2633.

[119] Yan T, Li S, Jiang W, Gao X, Xiang B, Voth GA, Structure of the Liquid–Vacuum In‐terface of Room-Temperature Ionic Liquids: A Molecular Dynamics Study. Journal of Physical Chemistry B 2006; 110(4) 1800–1806.

[120] Bhargava BL, Balasubramanian S. Layering at an Ionic Liquid-Vapor Interface: A Molecular Dynamics Simulation Study of [bmim][PF$_6$]. Journal of the American Chemical Society 2006; 128(31) 10073–10078.

[121] Sloutskin E, Lynden-Bell RM, Balasubramanian S, Deutsch M. The Surface Structure of Ionic Liquids: Comparing Simulations with X-ray Measurements. The Journal of Chemical Physics 2006; 125(17) 174715(1–7).

[122] Gannon TJ, Law G, Watson PR. First Observation of Molecular Composition and Orientation at the Surface of a Room-Temperature Ionic Liquid. Langmuir 1999; 15(24) 8429–8434.

[123] Law G, Watson PR. Surface Tension Measurements of N-Alkylimidazolium Ionic Liquids. Langmuir 2001; 17(20) 6138–6141.

[124] Law G, Watson PR. Surface Orientation in Ionic Liquids. Chemical Physics Letters 2001; 345(1-2) 1–4.

[125] Law G, Watson PR, Carmichael AJ, Seddon KR. Molecular Composition and Orientation at the Surface of Room-Temperature Ionic Liquids: Effect of Molecular Structure. Physical Chemistry Chemical Physics 2001; 3(14) 2879–2885.

[126] Baldelli S. Influence of Water on the Orientation of Cations at the Surface of a Room-Temperature Ionic Liquid: A Sum Frequency Generation Vibrational Spectroscopic Study. Journal of Physical Chemistry B 2003; 107(25) 6148–6152.

[127] Rivera-Rubero S, Baldelli S. Influence of Water on the Surface of Hydrophilic and Hydrophobic Room-Temperature Ionic Liquids. Journal of the American Chemical Society 2004; 126(38) 11788–11789.

[128] Fletcher KA, Pandey S. Surfactant Aggregation within Room-Temperature Ionic Liquid 1-Ethyl-3-methylimidazolium Bis(trifluoromethylsulfonyl)imide. Langmuir 2004; 20(1) 33–36.

[129] Bowers J, Vergara-Gutierrez MC, Webster JRP. Surface Ordering of Amphiphilic Ionic Liquids. Langmuir 2004; 20(2) 309–312.

[130] Bowers J, Butts CP, Martin PJ, Vergara-Gutierrez MC, Heenan RK. Aggregation Behavior of Aqueous Solutions of Ionic Liquids. Langmuir 2004; 20(6) 2191–2198.

[131] Iimori T, Iwahashi T, Ishii H, Seki K, Ouchi Y, Ozawa R, Hamaguchi H, Kim D. Orientational Ordering of Alkyl Chain at the Air/Liquid Interface of Ionic Liquids Studied by Sum Frequency Vibrational Spectroscopy. Chemical Physics Letters 2004; 389(4-6) 321–326.

[132] Sloutskin E, Ocko BM, Tamam L, Kuzmenko I, Gog T, Deutsch M. Surface Layering in Ionic Liquids: An X-ray Reflectivity Study. Journal of the American Chemical Society 2005; 127(21) 7796–7804.

[133] Halka V, Tsekov R, Freyland W. Peculiarity of the Liquid/Vapour Interface of an Ionic Liquid: Study of Surface Tension and Viscoelasticity of Liquid BmimPF$_6$ at Various Temperatures. Physical Chemistry Chemical Physics 2005; 7(9) 2038–2043.

[134] Hayashi S, Ozawa R, Hamaguchi H. Raman Spectra, Crystal Polymorphism, and Structure of a Prototype Ionic-liquid [bmim]Cl. Chemistry Letters 2003; 32(6) 498–499.

[135] Ozawa R, Hayashi S, Saha S, Kobayashi A, Hamaguchi H. Rotational Isomerism and Structure of the 1-Butyl-3-methylimidazolium Cation in the Ionic Liquid State. Chemistry Letters 2003; 32(10) 948–949.

[136] Neilson GW, Adya AK, Ansell S. Neutron and X-Ray Diffraction Studies on Complex Liquids. Annual Reports Section "C" (Physical Chemistry) 2002; 98 273–322.

[137] Abdul-Sada AK, Greenway AM, Hitchcock PB, Mohammed TJ, Seddon KR, Zora JA. Upon the Structure of Room Temperature Halogenoaluminate Ionic Liquids. Journal of the Chemical Society, Chemical Communications. 1986; 1753–1754.

[138] Lee BS, Chi YS, Lee JK, Choi IS, Song CE, Namgoong SK, Lee S. Imidazolium Ion-Terminated Self-Assembled Monolayers on Au: Effects of Counteranions on Surface Wettability. Journal of the American Chemical Society 2004; 126(2) 480–481.

[139] Wong DSH, Chen JP, Chang JM, Chou CH. Phase Equilibria of Water and Ionic Liquids [Emim][PF$_6$] and [Bmim][PF$_6$]. Fluid Phase Equilibria 2002; 194-197 1089–1095.

[140] Liu Y, Zhang Y, Wu G, Hu J. Coexistence of Liquid and Solid Phases of Bmim-PF$_6$ Ionic Liquid on Mica Surfaces at Room Temperature. Journal of the American Chemical Society 2006; 128(23) 7456–7457.

[141] Oh SH, Kauffmann Y, Scheu C, Kaplan WD, Rühle M. Ordered Liquid Aluminum at the Interface with Sapphire. Science 2005; 310(5748) 661–663; Hu J, Xiao XD, Ogletree DF, Salmeron M. Imaging the Condensation and Evaporation of Molecularly Thin Films of Water with Nanometer Resolution. Science 1995; 268(5208) 267–269.

[142] Chen S, Wu G, Sha M, Huang S. Transition of Ionic Liquid [Bmim][PF$_6$] from Liquid to High-Melting-Point Crystal when Confined in Multiwalled Carbon Nanotubes. Journal of the American Chemical Society 2007; 129(9) 2416–2417.

[143] Fitchett BD, Conboy JC. Structure of the Room-Temperature Ionic Liquid/SiO$_2$ Interface Studied by Sum-Frequency Vibrational Spectroscopy, Journal of Physical Chemistry B 2004; 108(52) 20255–20262.

[144] Romero C, Baldelli S. Sum Frequency Generation Study of the Room-Temperature Ionic Liquids/Quartz Interface, Journal of Physical Chemistry B 2006; 110(12) 6213–6223.

[145] Dupont J. On the Solid, Liquid and Solution Structural Organization of Imidazolium Ionic Liquids. Journal of the Brazilian Chemical Society 2004; 15(3) 341–350.

[146] Fukushima T, Kosaka A, Ishimura Y, Yamamoto T, Takigawa T, Ishii N, Aida T. Molecular Ordering of Organic Molten Salts Triggered by Single-Walled Carbon Nanotubes. Science 2003; 300(5628) 2072–2074.

[147] Lungwitz R, Spange S. Structure and Polarity of the Phase Boundary of N-Methylimidazolium Chloride/Silica. Journal of Physical Chemistry C 2008; 112(49) 19443–19448.

[148] Fukushima T, Kosaka A, Ishimura Y, Yamamoto T, Takigawa T, Ishii N, Aida T. Molecular Ordering of Organic Molten Salts Triggered by Single-Walled Carbon Nanotubes. Science 2003; 300(5628) 2072–2074.

[149] Mrozik W, Jungnickel C, Skup M, Urbaszek P, Stepnowski P. Determination of the Adsorption Mechanism of Imidazolium-Type Ionic Liquids onto Kaolinite: Implications for their Fate and Transport in the Soil Environment. Environmental Chemistry 2008; 5(4) 299–306.

[150] Joussein E, Petit S, Churchman J, Theng B, Righi D, Delvaux B. Halloysite Clay Minerals. Clay Minerals 2005; 40(4) 383–426.

[151] Levis SR, Deasy PB. Characterisation of Halloysite for Use as a Microtubular Drug Delivery System. International Journal of Pharmaceutics 2002; 243(1-2) 125–134.

[152] Guo B, Chen F, Lei Y, Liu X, Wan J, Jia D. Styrene-Butadiene Rubber/Halloysite Nanotubes Nanocomposites Modified by Sorbic Acid. Applied Surface Science 2009; 255(16) 7329–7336.

[153] El Abedin SZ, Polleth M, Meiss SA, Janek J, Endres F. Ionic Liquids as Green Electrolytes for the Electrodeposition of Nanomaterials. Green Chemistry 2007; 9(6) 549–553.

[154] Lockett V, Sedev R, Harmer S, Ralston J, Horne M, Rodopoulos T. Orientation and Mutual Location of Ions at the Surface of Ionic Liquids, Physical Chemistry Chemical Physics 2010; 12(41) 13816–13827.

[155] Sarangi SS, Raju SG, Balasubramanian S. Molecular Dynamics Simulations of Ionic Liquid–Vapour Interfaces: Effect of Cation Symmetry on Structure at the Interface. Physical Chemistry Chemical Physics 2011; 13(7) 2714–2722.

[156] Endres F, Höfft O, Borisenko N, Gasparotto LH, Prowald A, Al-Salman R, Carstens T, Atkin R, Bund A, El Abedin SZ. Do Solvation Layers of Ionic Liquids Influence Electrochemical Reactions? Physical Chemistry Chemical Physics 2010; 12(8) 1724–1732.

[157] Hayes R, Borisenko N, Tam MK, Howlett PC, Endres F. Atkin R. Double Layer Structure of Ionic Liquids at the Au(111) Electrode Interface: An Atomic Force Microscopy Investigation. Journal of Physical Chemistry C 2011; 115(14) 6855–6863.

[158] Frolov AI, Kirchner K, Kirchner T, Fedorov MV. Molecular-Scale Insights into the Mechanisms of Ionic Liquids Interactions with Carbon Nanotubes. Faraday Discussions. 2012; 154 235–247.

[159] Nakajima K, Ohno A, Hashimoto H, Suzuki M, Kimura K. Observation of Surface Structure of 1-Alkyl-3-Methylimidazolium Bis(Trifluoromethanesulfonyl)Imide Using High-Resolution Rutherford Backscattering Spectroscopy. The Journal of Chemical Physics 2010; 133(4) 044702 (1–7).

[160] Hashimoto H, Ohno A, Nakajima K, Suzuki M, Tsuji H, Kimura K. Surface Characterization of Imidazolium Ionic Liquids by High-Resolution Rutherford Backscattering Spectroscopy and X-ray Photoelectron Spectroscopy. Surface Science 2010; 604(3-4) 464–469.

[161] Lockett V, Horne M. Sedev R, Rodopoulos T, Ralston J. Differential Capacitance of the Double Layer at the Electrode/Ionic Liquids Interface. Physical Chemistry Chemical Physics 2010; 12(39) 12499–12512.

[162] Lin D, Liu N, Yang K, Zhu L, Xu Y, Xing B. The Effect of Ionic Strength and pH on the Stability of Tannic Acid-Facilitated Carbon Nanotube Suspensions. Carbon 2009; 47(12) 2875–2882.

[163] Maolin S, Fuchun Z, Guozhong W, Haiping F, Chunlei W, Shimou C, Yi Z, Hu J. Ordering Layers of [Bmim]PF$_6$ Ionic Liquid on Graphite Surfaces: Molecular Dynamics Simulation. The Journal of Chemical Physics 2008; 128(13) 134504 (1–7).

[164] Pinilla C, Del Popolo MG, Lynden-Bell RM, Kohanoff J. Structure and Dynamics of a Confined Ionic Liquid: Topics of Relevance to Dye-Sensitized Solar Cells. Journal of Physical Chemistry B 2005; 109(38) 17922–17927.

[165] Kislenko SA, Samoylov IS, Amirov RH. Molecular Dynamics Simulation of the Electrochemical Interface Between a Graphite Surface and the Ionic Liquid [BMIM][PF$_6$]. Physical Chemistry Chemical Physics. 2009; 11(27) 5584–5590.

[166] Mezger M, Schröder H, Reichert H, Schramm S, Okasinski JS, Schröder S, Honkimäki V, Deutsch M, Ocko BM, Ralston J, Rohwerder M, Stratmann M, Dosch H. Molecular Layering of Fluorinated Ionic Liquids at a Charged Sapphire (0001) Surface. Science 2008; 322(5900) 424–428.

[167] Kornyshev AA. Double-Layer in Ionic Liquids: Paradigm Change? Journal of Physical Chemistry B 2007; 111(20) 5545–5557.

[168] Sha M, Wu G, Fang H, Zhu G, Liu Y. Liquid-to-Solid Phase Transition of a 1,3-Dimethylimidazolium Chloride Ionic Liquid Monolayer Confined between Graphite Walls. Journal of Physical Chemistry C 2008; 112(47) 18584–18587.

[169] Shu W, Zhen C, Shu L, TianYing Y. A Molecular Dynamics Simulation of the Structure of Ionic Liquid [BMIM]PF$_6$/Rutile (110) Interface. Science in China Series B-Chemistry 2009; 52(9) 1434–1437.

[170] Zhang X, Cai Y. Octadecyltrichlorosilane (OTS)-Coated Ionic Liquid Drops: Micro-Reactors for Homogenous Catalytic Reactions at Designated Interfaces. Beilstein Journal of Nanotechnology. 2012; 3 33–39.

[171]   Chen F, Qing Q, Xia J, Li J, Tao N. Electrochemical Gate-Controlled Charge Transport in Graphene in Ionic Liquid and Aqueous Solution. Journal of the American Chemical Society 2009; 131(29) 9908–9909.